SAPIENZA
UNIVERSITÀ DI ROMA

Implementing physiologically-based approaches to improve Brain-Computer Interfaces usability in post-stroke motor rehabilitation

Research Doctorate (PhD program) in
"Automatica, Bioengineering and Operations Research"
cycle XXXI - Department of Computer, Control, and Management Engineering Antonio Ruberti

PhD Candidate — Eng. Emma Colamarino

Supervisor — Prof. Febo Cincotti
Co-supervisor — Dr. Donatella Mattia

Table of Contents

List of abbreviations

AUC	**A**rea **U**nder **C**urve
BCI	**B**rain-**C**omputer **I**nterface
Bic	**Bic**eps brachii muscle
CAR	**C**ommon **A**verage **R**eference
CNS	**C**entral **N**ervous **S**ystem
Del	Lateral **del**toid muscle
EEG	**E**lectro**e**ncephalo**g**raphy
EMG	**E**lectro**m**yo**g**raphy
Ext	**Ext**ensor digitorum muscle
Fle	**Fle**xor digitorum muscle
FMA	**F**ugl-**M**eyer **A**ssessment
FP/min	**F**alse **P**ositive per **min**ute
iLSDA	**I**ncremental updating of **L**ocality **S**ensitive **D**iscriminant **A**nalysis
iLSDA+LDA	**I**ncremental updating of **L**ocality **S**ensitive **D**iscriminant **A**nalysis followed by the **L**inear **D**iscriminant **A**nalysis

LDA	**L**inear **D**iscriminant **A**nalysis
lLAP	**l**arge surface **Lap**lacian
loBIP	**lo**ngitudinal **Bip**olar
LSDA	**L**ocality **S**ensitive **D**iscriminant **A**nalysis
LSDA + iLDA	**L**ocality **S**ensitive **D**iscriminant **A**nalysis followed by the **I**ncremental updating of **L**inear **D**iscriminant **A**nalysis
k-NN	**k**-**N**earest **N**eighbors Classifier
MAS	**M**odified **A**shworth **S**cale
MI	**M**ovement **I**magination
MRC	**M**edical **R**esearch **C**ouncil scale for muscle strength
MRCP	**M**ovement **R**elated **C**ortical **P**otential
MVC	**M**aximum **V**oluntary **C**ontraction
Pec	**Pec**toralis major muscle
ROC	**R**eceiver **O**perating **C**haracteristic
RMS	**R**oot **M**ean **S**quare
sLAP	**s**mall surface **Lap**lacian
SMRs	**S**ensori**m**otor **R**hythms

SW	**S**tep**w**ise
SWLDA	**S**tep**w**ise **L**inear **D**iscriminant **A**nalysis
TDR	**T**rue **D**etection **R**ate
trBIP	**tr**ansversal **Bip**olar
tri	**Tri**ceps brachii muscle

List of figures

List of tables

General introduction

Every two seconds, someone in the world experiences stroke [1]: an acute injury occurring in the brain caused by ischemia or haemorrhage. Stroke is one of the leading causes of long-term motor disability [2] and, as such, directly impacts on daily living activities. Therefore, identifying new strategies to recover motor function is a central goal of clinical research.

Driven by advances in technological areas, in the last years the approach to the post-stroke function restore has moved from the physical rehabilitation to the evidence-based neurological rehabilitation. The latter has its foundations in the principles of neuroplasticity, involved in growth as well as after acquired brain injury.

Brain-Computer Interface (BCI) technology offers the possibility to detect, monitor and eventually modulate brain activity. The potential of guiding altered brain activity back to a physiological condition through BCI and the assumption that this recovery of brain activity leads to the restoration of behaviour [3] is the key element for the use of BCI systems for therapeutic purposes.

To bridge the gap between research-oriented methodology in BCI design and the usability of a system in the clinical realm requires efforts towards BCI signal processing procedures that would optimize the balance between system accuracy and usability. My PhD thesis focuses on this issue. The aim is to propose new algorithms and signal processing procedures that, by combining physiological and engineering approaches, can provide the basis for designing more usable BCI systems to support post-stroke motor recovery.

Chapter 1
Brain-Computer Interfaces for post-stroke functional motor recovery

A brain-computer interface (BCI) is a system that measures central nervous system (CNS) activity and converts it into artificial output that replaces, restores, enhances, supplements or improves natural CNS output and thereby changes the ongoing interactions between the CNS and its external or internal environment [4].

My research activities focused on BCIs based on the electrophysiological phenomena occurring in the brain and recorded from the scalp (electroencephalography, EEG). Specifically, these BCI systems record the EEG signals, extract specific measures (features) from them and real-time convert them into output that act upon the outside world or the body itself (Figure 1).

During the last decades, different approaches have been proposed in BCI technology. A possible classification can be based on the control features used: single (brain) feature or multiple (brain-brain, brain-others) features.

Figure 1 - Overview of a BCI system. EEG signals, acquired from the scalp, are processed and analysed to extract specific signal features. These features are translated into commands that operate a device or feedbacks provided to the subject.

Single feature BCIs

Single feature BCIs are distinguished by the particular EEG (i.e. brain) feature that they use to control the system. This work focused on sensorimotor-rhythms and movement-related cortical potentials BCIs.

Sensorimotor-rhythms BCI

Sensorimotor rhythms (SMRs) are oscillations in the electric field recorded over the sensorimotor cortex. They typically fall into two major frequency bands: μ (8-12 Hz) and β (18-30 Hz). Voluntary movements are associated with μ and β event-related desynchronization (reduction in rhythmic activity related to an internally or externally paced event) localized over sensorimotor cortex [4] that can be measured using non-invasive BCIs (i.e. EEG-based BCIs).

Since mental practice in the form of movement imagination (MI) engages areas of the brain that govern movement execution, it has long been envisaged as a cognitive strategy to enhance post-stroke motor recovery [5]. Such reiterated engagement of motor areas is intended to influence brain plasticity phenomena, improving functional outcomes [6]. In this view, the combination of MI practice by means of SMRs-based BCI technology allows the access of the MI content under controlled conditions [7] thus, revealing the rehabilitative potential of MI.

At IRCCS Santa Lucia Foundation (Rome, Italy) the multidisciplinary team (neuroscientists, bioengineers and clinical rehabilitation experts) of the Neuroelectrical Imaging and BCI Lab conceptualized and developed a BCI prototype to support hand MI training in stroke patients [8]. The core of the device is a non-invasive EEG- based BCI which allows quantitative and controlled monitoring and reinforcement of EEG patterns generated by MI and provides patients with an ecologically enriched feedback: a realistic virtual representation of their own hands. At the same time, feedback about the patient's MI performance is provided to the therapist on a separate screen. This allows the therapist to monitor the patient's success in imagining the task and provide additional

feedback via verbal instructions/encouragement, resembling the setting of a traditional motor rehabilitation session.

To prove the clinical efficacy in improving hand functional motor recovery of the approach a randomized controlled clinical trial was performed [9]. Twenty-eight subacute unilateral, first ever stroke patients were recruited and randomly assigned to receive (as adjunctive to conventional physiotherapy) either a 1-month of MI-based BCI training or the same MI training with no (contingent) feedback (i.e., with no BCI-assisted). All patients were trained to perform MI of the affected hand movements, grasping and finger extension. Control EEG features for BCI training were selected by an expert neurophysiologist from the central and centroparietal electrodes located over the affected hemisphere that had shown desynchronization patterns (i.e. a decrease in spectral power) at EEG relevant (because modulated by the task) sensorimotor frequency. Reinforce the individual EEG patterns of reactivity that most resembled the physiological activation was the aim pursued through the BCI training. At completion of training, the BCI group showed a significantly greater improvement (Figure 2, left panel) in Fugl-Mayer scores [10], also accompanied by a significant increase of EEG motor-related oscillatory activity over the lesioned hemisphere.

The prototype in [9], engineered and implemented as an all-in-one BCI-supported MI training station, called Promotoer (Figure 2, right panel), is currently employed as add-on to standard therapy in one of the rehabilitation wards of IRCCS Santa Lucia Foundation (Rome, Italy).

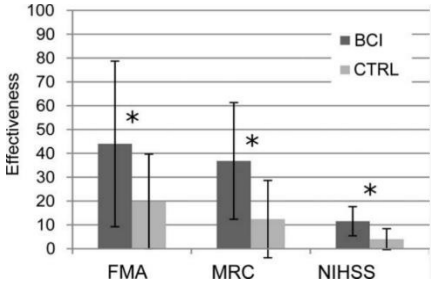

Figure 2 - Left Panel: [9] Bar diagram of the effectiveness of clinical outcome measures, Fugl–Meyer Assessment (FMA), Medical Research Council scale for muscle strength (MRC), National Institute of Health Stroke Scale (NIHSS), in the 2 groups (BCI and no-BCI-assisted groups). Asterisks mark significant differences between groups (independent-samples t test, $p < 0.05$). Right panel: The all-in-one BCI-supported MI training station, Promotoer, installed in a ward of the IRCCS Santa Lucia Foundation (Rome, Italy).

Movement-related cortical potentials BCI

Movement-related cortical potentials (MRCPs) are low frequency potentials associated with the planning and the execution of voluntary movements and measurable over the

sensorimotor cortex. They forerun the onset of actually executed movements as well as imagined movements [11] and occur both in cue-based or self-paced voluntary movements.

Since 2 seconds before the movement onset, indeed, a negative deflection (Figure 3) can be observed in the EEG signal; its peak of maximal negativity occurs closeness the onset of the movement [12]. The negative deflection consists of the readiness potential and the motor potential, associated with the planning/preparation [13] and the execution of the movement, respectively. The rebound phase, occurring after the peak of maximum negativity and also known as a movement-monitoring potential, is, instead, associated with the movement precision [14].

Since the initial negative phase of the MRCP can be detected before the onset of executed and imagined movements, MRCPs have been exploited to design rehabilitative protocols based on the principle of Hebbian associativity. According to Hebb, synapses that experience correlated activation of two different inputs are strengthened, whereas those weakened by uncorrelated activity are lost [15].

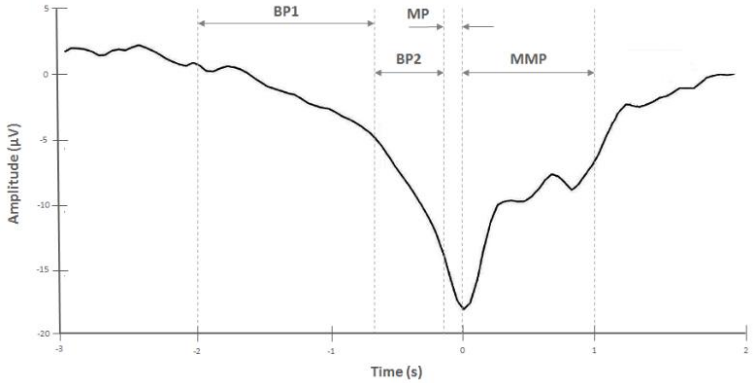

Figure 3 - Amplitude (μV) of the movement-related cortical potential (MRCP) as function of time (s): 0s corresponds to the movement onset. BP1 and BP2 are, respectively, early and late Bereitschaftspotential (readiness potential), MP, motor potential, and MMP, movement-monitoring potential.

This approach, implemented as a brain state-dependent peripherical stimulation protocol, was demonstrated to induce significant plasticity of the damaged cortex in stroke patients, translating directly into a functional improvement [16]. Briefly, once the MRCP was detected, the artificial activation of somatosensory afferents that project onto the motor cortex was triggered by means of non-invasive direct nerve stimulation. Peripheral nerve stimulation was timed to arrive at the motor cortex during the peak negative phase of the movement-related cortical potentials, inducing a causal relation

between the sensory signals arising from muscles involved in the movement and the physiologically generated brain wave during the movement imagination, attempt or execution. Only if the stimulation arrives during the peak negative deflection of the potential, it can lead to significant increasing in cortical excitability [17] and improvement in motor function.

Multiple features BCI

Recently, novel approaches based on more than one features have been proposed in BCI field. According to a recent review [18], information from

- two features of the brain signal,
- two different brain imaging methods,
- one feature of the brain signal and other physiological signal,
- one feature of the brain signal and another conventional input

has been combined in the framework of the so-called hybrid BCI.

In this thesis the combination of brain activity (i.e. EEG) and muscular activity recorded by the surface electromyography (EMG) is the meaning of the word hybrid BCI.

Hybrid EEG-EMG BCIs have been proposed in several BCI applications for communication or substitution: the signals can be fused as one input to the classifier or used independently, to ultimately increase the accuracy of the control [18], [19], [20], [21], [22].

In rehabilitative contexts, hybrid BCIs can combine residual EMG activity with motor-related brain activation and provide a contingent reward which aims at re-establishing the link between the CNS and the periphery that is disrupted by the stroke [23]. It has been shown that even in severely paralysed patients the residual EMG activity induced by motor attempt can be reinforced via a MI-based BCI training and then reliably used as a control signal in a further stage of rehabilitation [24]. Therefore, a modular approach, including different bioelectrical signals (EEG only, EEG combined with EMG) according to the patients' residual abilities and to the stage of recovery, could be envisaged.

Chapter 2
BCI technology translation to clinical realm

The research activity of three-years PhD program has been conducted in cooperation with the Neuroelectrical Imaging and Brain-Computer Interface Laboratory of the IRCCS Santa Lucia Foundation (Rome, Italy). It took advantage from the stimulating discussion with clinical experts (therapists and neurophysiologists). Therefore, in the context of supporting medicine (i.e. rehabilitative intervention post-stroke) with engineering methods, at the same time inspired by the physiological approaches, the fundamentals of this PhD thesis find the basis.

Thesis aim

Developing a flexible, usable and affordable BCI-driven device for post-stroke motor rehabilitation, that reinforces both brain patterns and residual muscular ability is the main goal of my project.

In this view two sub-goals were planned:

- investigate if improvements (new algorithms or new signal processing procedures) in the main blocks of the BCI system (pre-processing, feature extraction and translation, separately considered) can bring advantages in term of usability and affordability requirements;

- implement a procedure to analyse the residual muscle activity collected from stroke patients and extract the electromyographic features able to describe the *good* muscular recovery during rehabilitative intervention and follow each patient along the motor recovery process. From this point of view, the new device could be flexible and adaptable to different patients with variable degrees of impairment.

Thesis outline

The thesis consists of four main chapters.

In chapter 3, two studies will be presented and synthetically discussed. The first will introduce a new approach to the pre-processing of BCI data and compare it with the gold standard procedures applied to analyse EEG data collected during SMRs-based BCI protocol. The second will assess the impact of results obtained in the first study on BCI data collected from subacute stroke subjects performing hand MI tasks.

In chapter 4, one of the key points of the SMRs-BCI-assisted MI training will be investigated: the feature selection. The semiautomatic method developed to support the procedure will be described and compared with the current (*manual*) procedure applied by neurophysiologists.

After having investigated two first blocks of the BCI systems (signal pre-processing and feature extraction/selection), the impact of adaptive learning in the classification step will be assessed. In Chapter 5, three adaptive algorithms will be briefly described and compared with no-adaptive approach. While the key point of the SMRs-based BCI-assisted MI training in [9] is that the control feature doesn't change because its selection

and control is crucial for the rehabilitative purpose, there are some applications (i.e. MRCP detection) in which the efficacy of the rehabilitative intervention depends also on the ability of the BCI technology to adapt its parameters in time to comply the physiological changes occurring in the brain. For this reason, the study about adaptive learning was conducted on data collected from healthy subjects while performing the ankle dorsiflexion (typical task of MRCP-based BCI protocols).

In chapter 6, a preliminary analysis of EMG signals from 12 stroke patients will be performed. Changes in affected upper limb EMG pattern, after both stroke event and rehabilitative intervention, will be assessed to take inspiration to design the new EMG feature to control hybrid EEG-EMG BCI.

General conclusion will summarize the main key points of this PhD thesis.

Chapter 3
New approaches to BCI data pre-processing

Introduction

Spatial filters are generally designed to enhance sensitivity to particular brain sources, to improve source localization and/or to suppress artefacts. Most commonly, spatial filters are selected as a linear combination (i.e. weighted sums) of channels. There are several approaches for determining the set of spatial filter weights. These approaches fall into two major classes: data-independent and data-dependent spatial filters [4]. Data-independent spatial filters typically use fixed geometry relationships to determine the spatial-filter weights: they are based on physical consideration regarding how EEG signals travel through the skin and skull. Data-dependent spatial filters determine the weights directly from each BCI user's data; they can be classified into unsupervised data-driven (i.e. principal component analysis, PCA, or independent component analysis, ICA) and supervised data-driven filters (i.e. common spatial pattern, CSP) [25].

The proper selection of the spatial filter depends on the location and extent of the control signal and of the various sources of EEG or non-EEG noise.

In sensorimotor rhythms-based BCIs several approaches have already been proposed. Although recent studies propose the EEG data pre-processing by mean the CSP filter [26], [27], the surface Laplacian and the common average reference (CAR) are still among the most employed filters since they enhance the focal activity from the local sources and reduce the widely distributed activity [28]. Moreover, concerning the two variations of the Laplacian filter, i.e. the large and the small Laplacian, it appears that they are the best filters in target prediction and source identification, respectively [29].

This chapter focuses on data-independent spatial filters and proposes a new approach to the spatial filtering step in sensorimotor rhythms-based BCI that includes

- the introduction of bipolar derivations (commonly used in clinical EEG),
- the simultaneous use of more spatial filters,
- the relation between spatial filters and cortical regions.

Two studies were carried out: the first (Neurophysiological-based signal processing) aimed to investigate and characterize the proposed approach, the second aimed to evaluate the result impact on the SMRs-based BCI technology in supporting post-stroke motor rehabilitation.

Neurophysiological-based signal processing

EEG data, previously collected from thirty-nine healthy subjects during the motor execution and imagination of hand and feet movements, were analysed to compare the

a) performance of different spatial filters (commonly used spatial filters and bipolar derivations) as a function of the cortical region elicited by the experimental task,

b) performance of the spatial filters, previously considered, and that obtained by pooling information coming from different spatial filters together.

Materials and Methods

Data Collection

EEG data were collected from thirty-nine healthy subjects according the protocol and the procedure in [30]. Before the

inclusion in the study, approved by the IRCCS Santa Lucia Foundation (Rome, Italy) ethics committee, each subject gave written informed consent.

Briefly, EEG data were collected from 58, 59 or 61 electrodes assembled on a cap (according to an extension of the 10-20 International System, referenced to both ear lobes), amplified and sampled at 200 Hz (per channel) by a commercial EEG system (BrainAmp, Brain Products GmbH, Germany).

Subjects were comfortably seated in a reclining chair in a dimly lit room and instructed to minimize muscular, electrooculographic and blink activity. Subjects were asked to execute (first run) and imagine (second run) movements of both their hands (opening and closing) or feet (ankle dorsiflexion) upon the appearance (randomly) on the screen of top or bottom targets, respectively. The sequence was repeated three times for a total of six runs. Each trial (30 trials for each run) began when a target appeared on a side of the screen (Figure 4). The trial lasted 5.8 seconds, with the inter-trial interval of 1.8 seconds.

Figure 4 - Example of subject interface: subjects performed the execution or imagination (acquired in separate runs) of the ankle dorsiflexion (foot movement) when the target appeared in the bottom side of the interface. User interface designed by BCI2000 [31] software system.

Data Analysis

EEG data were offline analysed: band-pass filtered (0.1-70 Hz) with a forth order Butterworth filter and notch filtered at 50 Hz. The following spatial filters, conventional ear reference, common average reference, two Laplacian derivations (small and large) [28] and two bipolar derivations (longitudinal and transversal), were considered. In the bipolar derivations (applied via software) each voltage difference was computed between two channels, longitudinally subtracting e.g. FCz from Fz and transversely subtracting e.g. Cz from C1.

After the spatial filtering step, EEG data were divided into epochs 1 second long. The spectral analysis was performed on task epochs employing the maximum entropy method (16th order model, 2 Hz resolution, considering no overlapped epochs) [32]. All possible features (one for each couple

channel-frequency bin) in a reasonable range (i.e., 0-36 Hz) were extracted and analysed. A feature vector (spectral amplitude at each bin for each channel) was extracted from each epoch.

For the aim (a) movement execution runs were analysed. Since it was a SMRs-based BCI protocol, the analysis was constrained to features belonging to the sensorimotor strip (FC, C and CP channels) in the range from 7 Hz to 31 Hz (relevant frequencies). Moreover, hands opening/closing and feet flexion engage separate areas of the sensorimotor strip, different from both anatomical and functional point of view. Therefore, two scalp regions were considered: the hand area defined as the area containing FC, C and CP electrodes in all their even and odd positions (bilateral area); the feet area defined as the area containing electrodes placed on the midline, e.g. FCz.

Features belonging to each area were the input for the stepwise regression [33] whereby the subset of features and weights, optimal to build an effective regression model to evaluate the relationship between the features and the dependent variable (here equivalent to subject's movement), was identified. The maximum number of features to be selected by the stepwise regression algorithm was set, for all feature domain (one

domain for each spatial filter), to eight accordingly to the results obtained in a preliminary study (not reported in this thesis). The latter aimed to compute the optimal number of features above which the classification performance average (across tasks and subjects) didn't grow in a significant way. Results showed that increasing the number of features (above eight) did not result in significantly better performance values.

A linear approach (stepwise linear discriminant analysis, SWLDA, [34]), based on the combination of features and weights returned by the stepwise regression, was applied for the classification of the EEG epochs. A 15-fold cross-validation design was implemented and classification performance in term of the area under the Receiver Operating Characteristic (ROC) [35] curve were assessed for each feature domain (one for each spatial filter applied).

For the aim (b) execution and imagination runs were analysed. Only twenty-eight subjects performed both executed and imagined movements. For this analysis, features from both hand and foot areas were considered together as a single feature domain. Therefore, the analysis included six feature domains, each one extracted from EEG signals pre-processed by one of six filters earlier defined, and a new feature domain

obtained by pooling EEG features from longitudinal and transversal bipolar filters together. The performance assessment followed the same stages in (a).

Statistical Analysis

For each spatial filter, the Shapiro-Wilk test was applied to assess the normality of the performance value distribution. To investigate the performance of different spatial filters in relation to the scalp area (aim a), classification performances (in movement execution runs) were analysed by means an ANOVA statistical design, the repeated measures two-way analysis of variance: six levels (six filters earlier listed) for the spatial filter factor, two levels (hands and feet) for the area factor.

To the aim (b), classification performances were analysed by means the two-way ANOVA statistical test (repeated measures): seven levels for the filter factor (6 filters listed earlier and the new filter obtained combining longitudinal and transversal bipolar filters information) and two levels for the modality factor (movement execution and imagination). The Tukey HSD post hoc analysis was conducted to assess pairwise differences. For all statistical analysis, threshold for statistical significance was set to $p < 0.05$. All results are presented as mean ± SE (standard error) across subjects.

Results

Figure 5 shows the classification performances (area under the ROC curve) of the considered spatial filters as a function of the cortical region elicited by the experimental task. The repeated measures two-way ANOVA revealed a significant effect of both spatial filter ($F=24.85$, $p < 0.01$) and scalp area ($F=17.73$, $p < 0.01$) factors and a significant area–filter interaction ($F=7.43$, $p < 0.01$).

All spatial filters perform better than the ear-reference method confirming the results in [28]: common average reference and large surface Laplacian spatial filters are significantly superior to the ear-reference method. Filter EEG signals by means of transversal/longitudinal bipolar filters isn't different from not applying filters if hand/feet areas are considered, respectively. Moreover, while longitudinal bipolar filter shows performances as good as the common average reference for the hand scalp area, the transversal bipolar filter seems, on average, outperforms the common average reference and even the small Laplacian derivation in feet area.

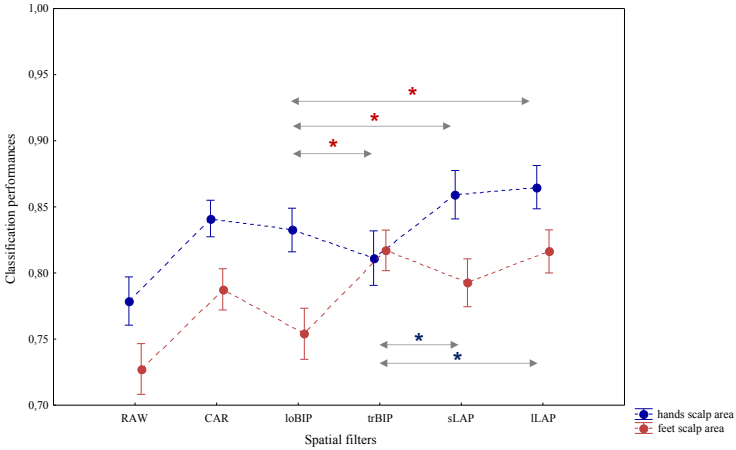

Figure 5 - Classification performances (area under the ROC curve) are expressed as mean ± SE (standard error, n=39 healthy subjects) and computed for each spatial filter: ear reference (RAW), common average reference (CAR), longitudinal bipolar (loBIP) and transversal bipolar (trBIP) filters, surface Laplacian in its small (sLAP) and large (lLAP) derivation. Asterisks (*) mark significantly different pairs identified by the post hoc test. Features used in the classification step were selected from the hand (blue) and the foot (red) scalp areas by means the stepwise regression. The differences pointed out in the post-hoc test are marked accordingly. Although the figure does not report (to not reduce the figure readability) the comparison between RAW and others filters, all filters differ from ear-reference, except for the trBIP/ loBIP in the hands /feet scalp area, respectively.

Figure 6 shows the classification performances (area under the ROC curve) of the considered spatial filters as a function of the task modality (movement executed or imagined). The repeated measures two-way ANOVA revealed a significant effect of both spatial filter ($F=19.98$, $p < 0.01$) and modality ($F=45.96$, $p<0.01$) factors and no significant filter-modality interaction ($F=2.03$, $p= 0.064$).

The results confirm the findings in [29]: the large surface Laplacian is one of the best spatial filtering approach in target prediction. Pooling EEG features from longitudinal and transversal bipolar filters together seems, on average, perform better than each spatial filter considered individually. However, while longitudinal and transversal bipolar filters significantly differ from large surface Laplacian, no significant differences appear between the two Laplacian derivations (small and large) and the new domain (lo+tr)BIP, even when movements were imagined. Moreover, in the latter, even if each bipolar filter doesn't statistically differ from the ear-reference spatial filter, pooling bipolar domains together outperforms the RAW filter.

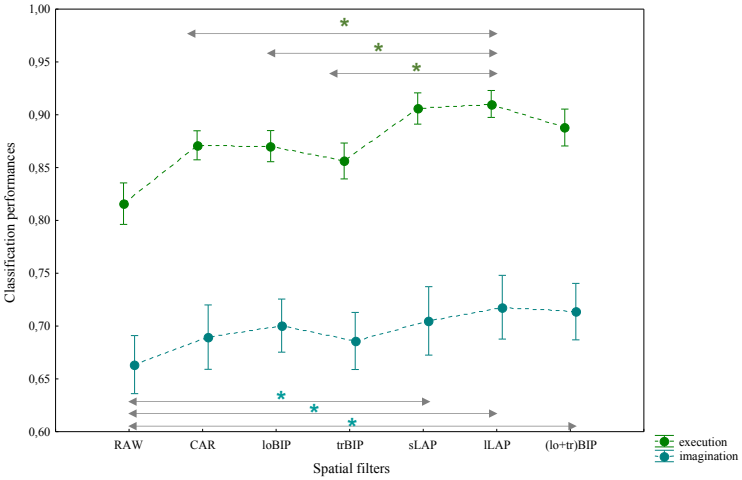

Figure 6 - Classification performances (area under the ROC curve) are expressed as mean ± SE (standard error, n=28 healthy subjects) and computed for each spatial filter: ear reference (RAW), common average reference (CAR), longitudinal bipolar (loBIP) and transversal bipolar (trBIP) filters, surface Laplacian in its small (sLAP) and large (lLAP) derivation and the filter obtained by pooling EEG features from bipolar domains together (lo+tr)BIP. Asterisks (*) mark significantly different pairs identified by the post hoc test. The evaluation was performed for the executed (green) and imagined (light blue) movement runs. The differences pointed out in the post-hoc test are marked accordingly. Although the figure does not report the comparison between RAW and others filters, all filters differ from ear-reference when the movement was executed.

As a proof of concept, in Table 1 are presented features selected in the new domain (obtained pooling EEG features from bipolar filters together) and those selected in the small Laplacian domain for three subjects (same classification performances for both spatial filters). Results suggest a reduction of the number of electrodes needed to extract the features passing from the small Laplacian filter to the new domain.

Table 1 - List of the features (feature: channel-frequency) selected in small surface Laplacian (sLAP) and (lo+tr)BIP feature domains. No statistical difference for this pair of filters from the previous analysis (aim b). Three representative subjects (S01, S02, S03) were considered for the comparison. The classification performances, for each subject, are the same for both filters. Channels positions are conformed with 10-20 International System. Each channel indicated in sLAP is the central electrode of the difference (e.g., C3 is the central electrode: the surface Laplacian involved its neighbors C1, C5, FC3, CP3). NE is the number of electrodes needed to realize the hardware montage.

	S01				S02				S03			
	sLAP		(lo+tr)BIP		sLAP		(lo+tr)BIP		sLAP		(lo+tr)BIP	
	chan – freq (Hz)		chan – freq (Hz)		chan – freq (Hz)		chan – freq (Hz)		chan – freq (Hz)		chan – freq (Hz)	
1	C3	11	FC3-C3	11	CP4	11	FC4-C4	11	C4	13	FC3-C3	13
2	Cz	27	Cz-C2	13	CPz	25	CP4-P4	25	CP3	13	C2-C4	13
3	C4	13	Cz-CPz	29	C4	25	CPz-Cz	25	Cz	25	F5-FC5	17
4	C4	21	CPz-Pz	21	C3	13	C1-Cz	11	C6	11	TP7-CP5	27
5	Cz	21	FC3-C3	17	C2	29	CP3-P3	27	FC5	29	FC6-C6	13
6	FC3	31	FC1-C1	11	FC3	15	CP1-CPz	25	C3	13	C1-Cz	25
7	FC2	25	FC4-C4	21	CP4	25	FC4-C4	25	CP3	15	FC4-FC6	31
8	CP6	13	C1-Cz	11	Cz	27	F5-FC5	19	C6	27	CPz-CP2	29
NE	21		10		22		12		22		15	

Discussion

Spatial filtering is a crucial step to ensure optimal BCI system performances. In this study the spatial filters (data independent spatial filters) commonly used in BCI control were compared with filters commonly used in EEG clinical application (e.g., bipolar filters). Moreover, the relation between performances shown by several (BCI and clinical gold standard) spatial filters and the sensorimotor strip areas, engaged in different movements, was investigated. Consider scalp areas separately (i.e., hands area and feet area) highlights interesting differences (e.g., from longitudinal and transversal bipolar in the feet area) that haven't emerged considering features in the whole sensorimotor strip. Moreover, if on the one hand the longitudinal filtering doesn't significantly differ from the gold standard filters (surface Laplacian) in the hand area, on the other hand the same trend is shown by the transversal filtering in the feet area, carrying to hypothesize a relationship between the direction of the bipolar filter yielding the highest performance and the specific cortical region elicited by the experimental task. The identification of the best spatial filter could be, therefore, related to the scalp area (its anatomical and functional properties) of interest and thus, improving performance can be pursued using specific filters for specific

areas. Further analysis will be oriented to investigate the reason why transversal bipolar filter shows better performance in the feet area. In addition, these findings require a consolidation by exploring their use with other motor tasks (different from hand opening/closing and feet flexion) and/or imagined movements.

Integrating feature information or, specifically, pooling EEG features from bipolar (longitudinal and transversal) filters together, improves (on average) the classification performance respect to that obtained considering each domain individually. No differences were found between the performance obtained by the integrated approach and those obtained by the surface Laplacian filters (i.e., the gold standard when scalp areas were considered all together). Moreover, a preliminary comparison of the number of electrodes needed to realize the hardware montage, containing just the appropriate features selected for the rehabilitation, suggests that the use of a new integrated approach for feature extraction has the potential to reduce setup time and, therefore, enhance the usability of the BCI technology.

Impact on SMRs-based BCIs stroke rehabilitation

In the previous study, we observed that in a cursor control task (hand vs foot movement) processing hand scalp-area EEG data with longitudinal bipolar filters (loBIP) returns better classification performances than those of the transversal bipolar filters (trBIP). Hypothesizing that the former would return better results in all hand movement-based paradigms, we aimed at comparing

a) the classification performance of commonly used spatial filters, bipolar filters and the combination of both bipolar filters obtained by pooling EEG features together,

b) the number of electrodes needed as consequence of the spatial filter choice,

analysing EEG data collected from fifteen subacute stroke subjects during the imagination of hand movements (vs rest).

Materials and Methods

Data Collection

EEG data were collected from fifteen stroke subjects according the procedure and the protocol in Appendix B. Briefly, EEG data were collected from 61 electrodes assembled on an electrode cap according to an extension of the 10–20 International System, sampled at 200 Hz and notch filtered (50 Hz). All subjects were trained to perform the motor imagery of the hand movements (grasping and finger extension) with their unaffected and affected upper limbs (recorded in separate runs). Each run comprised 30 trials (15±1 rest, 15±1 motor imagery). The total duration of each trial was 7 seconds.

Data Analysis

Ocular artefacts were removed by independent component analysis [36]. EEG signal intervals containing artefacts (muscular, environmental) were identified, using a semi-automatic procedure, based on the definition of a voltage threshold, and discarded.

Recordings collected during the motor imagery of grasping and finger extension were concatenated. To consider the same number of samples for each condition (rest or task), the last 4

seconds of each trial were considered (i.e. while in rest trials subjects were in rest condition for 7 seconds, in task trials 3 seconds in rest condition come before 4 seconds of movement, see Figure in appendix B to detailed explanation).

For aim (a) the following spatial filters were considered: CAR61 (CAR computed on all recorded channels); CAR31 (CAR on 31 electrodes, FC-C-CP-P-PO); lLAP (large surface Laplacian); loBIP (interelectrode distance: 3 rows, e.g. FCz-Pz); trBIP (interelectrode distance: 2 columns, e.g. Cz-C3) and (lo+tr)BIP (pooled features).

EEG data collected in each experimental condition (unaffected hand MI and affected hand MI) were divided into epochs 1 second long and spectral features (spectral amplitude at each bin for each EEG channel) were extracted using the maximum entropy method (16th order model, 2 Hz resolution, no overlap) [32]. Given the specific motor rehabilitation context, spectral features belonging to the sensorimotor strip in the contralateral area to the hand involved in the task and in the range from 7 Hz to 25 Hz were used for the classification (step-wise linear discriminant analysis [34], [37]). Classification performances in term of area under the Receiver Operating Characteristic (ROC)

[35] curve were assessed using a 20-fold cross-validation design.

For aim (b) for each spatial filter the minimum number of physical electrodes that would be needed to extract the features identified by the stepwise algorithm in (a) as the best set required by the classifier was computed. Specifically, for each feature domain (one for each spatial filter) the stepwise method selected among the subset of features coherent with the specific application (SMRs-based BCI to support motor rehabilitation protocols) the statistically significant features to use for the classification step. The number of electrodes to record EEG data needed to extract those features was computed.

Statistical Analysis

Shapiro-Wilk tests were applied to assess the normality of the performance value distribution. To investigate the performances of different spatial filters, classification performances were analysed by repeated measures one-way analysis of variance (ANOVA). The Tukey HSD post hoc analysis was applied to assess pairwise differences. The threshold for statistical significance was set to $p<0.05$. Results are presented as mean ± SE (standard error).

Results

Statistical analysis revealed, in each condition, a significant effect of the spatial filter factor ($F(5, 70) = 4.35$, $p < 0.01$ unaffected hand, $F(5, 70) = 2.42$, $p = 0.04$ affected hand). Figure 7 shows the statistical analysis output and post-hoc test results. All spatial filters showed average classification performances higher than 0.8, with a similar trend for unaffected and affected hand. Common average reference spatial filter performed as well as the large surface Laplacian confirming, although in a different task, the result in [28]. Longitudinal bipolar filter performed as well as the common average reference and the surface Laplacian spatial filters. The statistical differences, pointed out by the post-hoc test, confirmed the results of the previous study. Pooling EEG features from both longitudinal and transversal bipolar filters together led to a significant better result than the transversal bipolar filter and, on average, than that of the surface Laplacian.

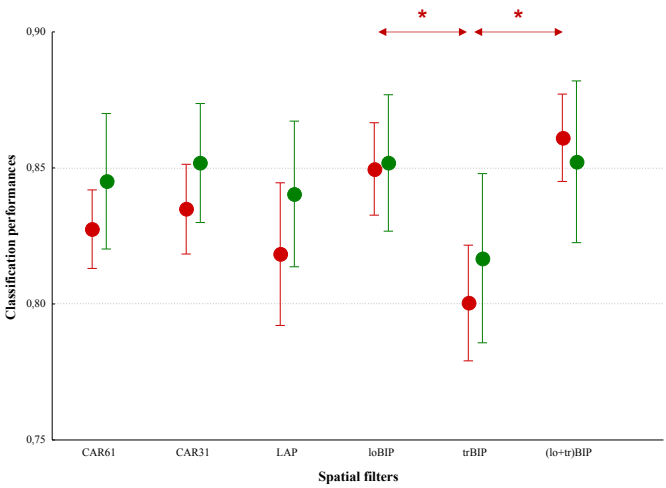

Figure 7 - Classification performances (area under the ROC curve values) are expressed as mean ± SE (standard error; n=15 patients) and computed for each spatial filters: common average reference on all recorded channels (CAR61), common average reference on 31 channels (CAR31), large surface Laplacian (LAP), longitudinal bipolar filters (loBIP), transversal bipolar (trBIP) filters and that obtained by pooling EEG features from bipolar domains together (lo+tr)BIP. Asterisks (*) mark significantly different pairs identified by the post hoc test. Red and green markers refer to the motor imagery of unaffected and affected hand respectively.

In Figure 8 the number of electrodes needed to extract the features required by the trained classifier are illustrated. Apply the common average reference requires all collected channels (61 EEG electrodes). Consider a “smaller” version of the common average reference, including electrodes in centre-parietal scalp area, didn’t differ in term of classification performance from the whole configuration, even if fewer number of electrodes is required. Even if the surface Laplacian, the longitudinal bipolar and the combined spatial filter did not differ among them (Figure 7), the longitudinal bipolar filter seems the best filter to reduce the number of EEG electrodes.

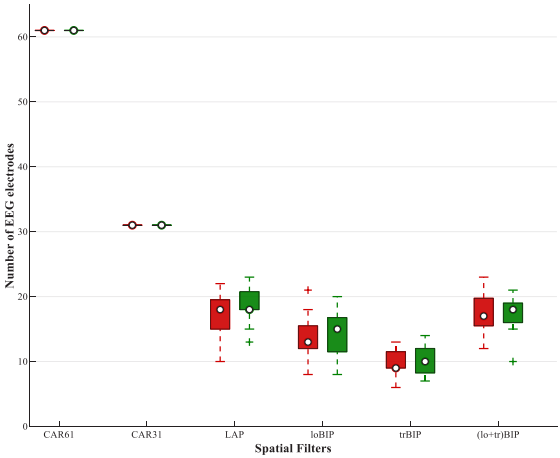

Figure 8 - Box plots of the number of electrodes needed to collect EEG signals and extract from them the features required by the classifier to reach the performance shown in Figure. Common average reference on all recorded channels (CAR61), common average reference on 31 channels (CAR31), large surface Laplacian (LAP), longitudinal bipolar filters (loBIP), transversal bipolar (trBIP) filters and that obtained by pooling EEG features from bipolar domains together (lo+tr)BIP are the spatial filters applied on EEG data collected while subjects performed hand movements with their unaffected (red) and affected (green) hand.

Discussion

Results suggest that the classification performances of longitudinal bipolar filter (commonly used in the clinical EEG) are as high as common average reference (the most frequently used). Moreover, the former required a significantly lower number of physical EEG electrodes to compute the features needed by the trained classifier. Among bipolar filters, longitudinal bipolar filter performed better than transversal bipolar filter, confirming the results shown in the previous study about the relationship between the direction of the bipolar filter (e.g. longitudinal rather than transversal bipolar) and the specific cortical region elicited by each experimental task (e.g. hand MI). Pooling EEG features, extracted applying both longitudinal and transversal bipolar filters, together yielded significantly higher classification results than those of the transversal but it didn't improve the good longitudinal bipolar filter performance suggesting that information from the transversal bipolar derivations was considered by the classifier redundant information.

Main message

Minimizing the number of electrodes is key to transfer BCIs to clinical use, making them more affordable (lower equipment cost), more efficient (reduced setup time), and more usable (less burden for therapist and patient). The optimization of the signal processing procedure is a crucial step to achieve this goal, while preserving the effectiveness (accuracy) of the output.

The relation between the direction of the bipolar filter and the specific cortical region elicited by each experimental task suggests that useful information for optimal feature extraction in SMRs-based BCIs can be obtained taking into account neurophysiological aspects.

Though the marginal improvement in classification performances of longitudinal bipolar filters over common average reference (most frequently used) does not reach statistical significance, the significant reduction of the number of electrodes needed for the longitudinal bipolar filters suggests that the new approach, based on bipolar signals-based feature extraction, has the potential to enhance the usability of the BCI technology in post-stroke motor rehabilitation of the upper limb.

Chapter 4
Semiautomatic-physiologically-driven BCI control parameter selection

Introduction

SMRs-based-BCI-assisted motor imagery training has been demonstrated to be effective in post-stroke motor recovery of the upper limb function. Through BCI training, the researchers aimed to reinforce the individual EEG pattern of reactivity that most resembled the physiological activation that was relevant to movement imagination of the affected hand [9]. Reinforce a specific pattern (related to MI) meant provide patients with a feedback related to a specific sensorimotor activity (frequency content) located in a certain sensorimotor area and, therefore, choose appropriate BCI control parameters (EEG features).

In the study presented by Pichiorri et al. [9], EEG features, channels and frequencies, were identified according to a *manual* procedure (following EEG data analysis of the calibration session). Namely, neurologists and/or therapists identified the features taking into account neurophysiological evidence and rehabilitation principles: relevant control features were selected from the central and centroparietal electrodes

that were distributed only over the affected hemisphere that showed desynchronization patterns (i.e., a decrease in spectral power) at EEG frequencies that were typical for the modulation of sensorimotor rhythms. The selection was based on the visualization of matrices obtained from the features' statistical comparison between two conditions (motor imagery task and rest).

In that way, the procedure is highly dependent on the operator and is not suitable for the majority of therapists because it requires experience for visualizing patterns of desynchronization in that form and specific neurophysiological knowledge. To overcome these limitations, we developed a semiautomatic method to select control features that combines both machine learning and physiological approaches.

Feature selection is a crucial step in BCI, since it directly impacts on the system performance. It allows to exclude redundant features or those not related to the mental states targeted by the BCI, to reduce possible overtraining effects, increase the computational efficiency of the classifier. Feature selection methods can be categorized in three approaches: filter, wrapper and embedded approaches. Filters methods rely

on measure of relation between each feature and the target class. They are classifier-independent and very fast (linear complexity) but they may lead to a selection of redundant features. Wrapper and embedded approaches overcome this limitation but needed a longer computation time. Wrapper methods select a subset of features and evaluate the subset effectiveness observing the performance of the classifier trained and tested by those features. Embedded methods merge the feature selection and the evaluation in a unique process (e.g. the decision tree or the stepwise linear discriminant analysis) [25]. In SMRs-based BCIs the maximal mutual information algorithms [38], the recursive feature elimination algorithms based on the training of a support vector machine classifier [39] and the genetic algorithms [40] have been proposed as feature selection methods in both binary and multi-class classification. Moreover, other procedures [41], based on the stepwise multiple regression, have been applied to periodically update the features used to control cursor movement across training sessions.

Due to the good results obtained by the stepwise regression and because in our design a linear classifier (fast and simple from the in interpretative point of view) would have been preferred, we chose to found our methods on an embedded

(supervised) feature selection method as the stepwise linear discriminant analysis.

The inclusion of neurophysiological constraints is the key of our improvement. Moreover, in view of a wider employ of the BCI-based rehabilitation in stroke, a user-friendly graphical interface, GUIDER, was developed to guide the operator in the feature selection procedure, giving him the possibility to interact with the algorithm to define new additional physiological constraints for the selection procedure.

In the overview [42] of publicly available software platforms for BCIs, the presented tool might match needs of rehabilitation BCI researchers orientated to a translational approach, from machine learning to physiology and vice-versa.

After a brief description of the method and the GUIDER tool, this chapter proposes the comparison of the manual procedure (by skilled user) and the guided procedure (by the developed method) in term of both selected features and classification performances.

Materials and Methods

GUIDER - User interface description and operating procedure

GUIDER is a graphical user interface (GUI) for semiautomatic and physiologically driven EEG features selection. It was designed and developed in MATLAB R2015a (The MathWorks, Inc., Natick, Massachusetts, USA). GUIDER (Figure 9) allows users to interact with BCI data through a graphic interface without needing to use MATLAB syntax.

Specifically, it allows to (i) import BCI data and montage files, (ii) process EEG data applying spatial and frequency filtering, (iii) extract EEG spectral features, (iv) visualize the EEG patterns of desynchronization in the form of statistical index matrices.

The operator can choose which feature selection to apply. Three feature selection modalities are allowed by GUIDER, each for a specific user skill and experience level in BCI data analysis and in rehabilitative protocol principles.

Figure 9 - GUIDER interface

Choosing the

- Guided modality, the operator has to flag just the affected hemisphere (to involve in the rehabilitation program) and EEG channels (all belonging to the sensorimotor strip) to include in the analysis performed by the developed method;

- Semi-Guided modality, the operator has to define topographical constrains for the developed automatic method, drawing some areas into the statistical matrix;

- Manual modality, the operator chooses to identify the EEG feature directly from the visual inspection of the statistical matrix.

GUIDER returns three files, a text file, an excel file and an external parameter file (ready to be loaded on BCI2000 [31] system for the BCI training session). All files contain information about selected features and their weights (assigned by the automatic method).

GUIDER was designed according to the principles of the user-centred design approach [43]. Neurologists, therapists and no-skilled users were enrolled and involved in all stages of the project in order to understand user specific requirements, the whole user experience and the context of use. In each meeting the evaluation of the usability, effectiveness and efficiency of the tool provided the bases for the discussion between developer and users.

GUIDER – semiautomatic, physiologically-driven BCI control parameters selection method

Since the rehabilitative approach, proposed in [9], aimed to reinforce the individual EEG pattern that most resembled the physiological activation, relevant to movement imagination of

the affected hand, our feature selection method includes physiological constraints related to the spectral and spatial distribution of the sensorimotor activity elicited by the motor imagery task in the calibration session (preliminary to the BCI training). While spatial (topographic) constraints in the affected hemisphere can be defined by the user through the Guided or the Semi-Guided procedures, spectral constraints are fixed in the range [7 25] Hz because of the frequency bands (μ and β) that characterize the sensorimotor rhythms. In this way, physiological constraint definition aims to take into account neurophysiological evidence and rehabilitation principles, according to which the control features have been the same for all BCI training sessions.

The algorithm is based on the stepwise regression [33]. It identifies an optimal subset of predictor variables (i.e. the features) and assigns weights to them in order to build an effective regression model to evaluate the relationship between the predictors and the dependent variable (here equivalent to subject's intention, e.g. task vs rest). Starting with an empty model, for each iteration the algorithm

a) adds (or removes since the third iteration) a feature to (from) the classification model in order to obtain a

combination of features ensuring a good classification performance;

b) checks if an EEG pattern of synchronization or desynchronization occurs for that feature (discarding it if a synchronization pattern occurs),

c) checks if there is a common characteristic (i.e. same EEG channel or frequency) between the new feature and the features already included in the model. If exists and it is the EEG channel, the algorithm includes the feature in the model, not increasing the counter that stops the algorithm when the maximum number of physical electrodes available in the training setup is reached.

The algorithm stops when, adding features, the accuracy of the model doesn't improve in the statistical sense.

In the following study, the comparison between manual and guided procedures is presented.

For the feature selection step both manual and guided procedures were applied using the developed tool (GUIDER). Because the manual procedure requires experience in BCI field and specific neurophysiological knowledge, an expert neurophysiologist was enrolled to run the procedure. To run the

guided procedure a no-skilled user was enrolled and instructed for each dataset (one for each stroke subject) to flag the hemisphere affected and all EEG channels available in the interface (i.e. FC, C and CP). The same datasets were presented to the users.

Features selected by the expert neurophysiologist and by the no-skilled user were collected and used to compute offline (later respect to the feature selection process) the classification performance.

Data Collection

For the feature selection step, EEG data, collected during the Pre-Intervention session from thirteen stroke subjects (who received the BCI-assisted MI training intervention, see appendix B for further details) according the procedure and the protocol in Appendix B (Pre-Intervention assessment), were analysed. Briefly, EEG data were collected from 61 electrodes assembled on an electrode cap according to an extension of the 10–20 International System, sampled at 200 Hz and notch filtered (50 Hz). All subjects were trained to perform the motor imagery of the hand movements (grasping and finger extension, recorded in separate sessions) with their affected upper limb. Each run

comprised 30 trials (15±1 rest, 15±1 motor imagery). The total duration of each trial was 7 seconds.

For the classification performance assessment, to reproduce the most realistic scenario of the rehabilitation program EEG data recorded during the first training session (planned later respect to the calibration session) were analysed. EEG data were collected from the same subjects previously considered, according to the procedure and protocol in Appendix B, Intervention assessment. Briefly, EEG data were recorded from 31 electrodes distributed over the scalp centroparietal region. All data were sampled at 200 Hz. The training session comprised two runs (one for each motor imagery task, grasping and finger extension). Each run comprised 20 trials and each trial included a rest period of 4 seconds and a task period of maximally 10 seconds. During the task period, patients were asked to perform only the MI of the affected hand [44].

Data Analysis

For both aims (feature selection and classification performance assessment) runs collected during the motor imagery of grasping and finger extension were concatenated.

For the feature selection step, GUIDER was programmed to

- filter EEG signals by the common average reference spatial filter;
- segment EEG signals in epochs 1 second long;
- extract for each epoch spectral features (spectral amplitude at each bin for each channel) using the maximum entropy method (16th order model, 2 Hz resolution, no overlap) [32];
- assess modulation induced on a specific feature by the task, computing for each feature the coefficient of determination R-square;
- plot EEG patterns of desynchronization in the form of statistical index matrix.

For each dataset, a matrix was presented to the user. To compare the procedures, we defined as two the maximum number of valid EEG features and programmed GUIDER accordingly (for the guided procedure). For the manual procedure the expert neurophysiologist was invited to select two features and assign them weights.

For the classification performance assessment, EEG data collected during the first training session were analysed offline

according to a similar procedure (common average reference spatial filtering, segmentation and spectral feature extraction using the maximum entropy method). The output of the linear combination of the selected features and weights (separately for both manual and guided procedures) was used to compute the Receiver Operating Characteristic (ROC) curve [35]. The area under the ROC curve was the index used to assess the classification performance.

Statistical analysis

After having assessed the normality of the performance value distributions (Shapiro-Wilk tests), classification performance values (manual vs guided procedure) were compared by a paired-samples t-test. The threshold for statistical significance was set to $p<0.05$.

Results

Figure 10 shows a typical graphic output of GUIDER: it displays (subject #7) the R-square values of all features (61 channels and 18 frequency bins) after the common average reference (CAR) filtering.

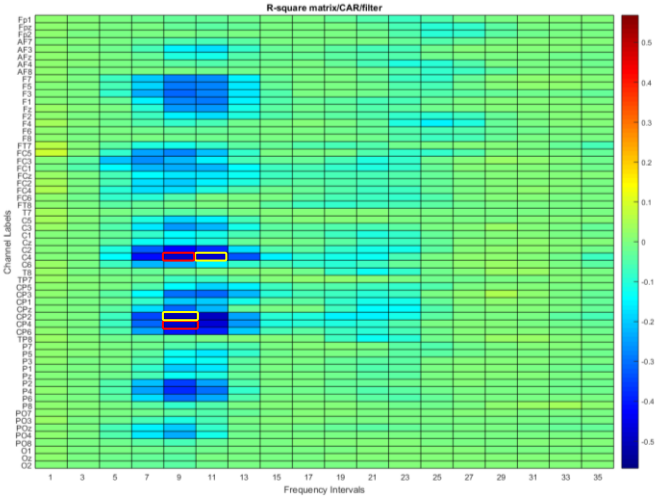

Figure 10 - R-square matrix (channels and frequency intervals) obtained from EEG data collected during the Pre-intervention session from a subacute stroke subject with right-sided lesions (subject #7). The red (channels CP4 and C4 at 9 Hz) and yellow rectangles (channels CP2 and C4 at 9 Hz and 11 Hz, respectively) are features selected by an expert neurophysiologist (manual procedure) and no-skilled user (guided procedure), respectively.

The relevant control features selected, just basing on the R-square matrix visualization by an expert neurophysiologist and those identified by the guided procedure (based on the developed method), are reported in Table 2. For most of subjects (except #6, #7, #8, #10) both procedures returned the same first feature in term of both topographic and spectral characteristics. Since the developed method ranked features according the statistical significance, the neurophysiologic was asked to apply a similar procedure, identifying as first the most important feature. For the subject #2 the similarity of topographic characteristic (i.e. C2) coexisted with a different spectral characterization (21 Hz instead of 23 Hz).

Table 2 - BCI control features identified from EEG data collected in the Pre-intervention session (for all subjects) by an expert neurophysiologist (manual procedure) and by a no-skilled user (guided procedure). For each feature, EEG channel and frequency are reported in the left and right columns for the manual and guided procedures, respectively.

ID	Hemisphere affected	Control features	Manual procedure		Guided procedure	
			EEG channel	Frequency (Hz)	EEG channel	Frequency (Hz)
#1	Right	1	CP4	17	CP4	17
		2	C6	11	C6	9
#2	Right	1	C2	23	C2	21
		2	CP2	23	Cz	25
#3	Left	1	C1	9	C1	9
		2	CP3	9	FC3	9
#4	Left	1	C3	13	C3	13
		2	CP3	13	Cz	19
#5	Right	1	C4	9	C4	9
		2	CP4	9	FC4	15
#6	Right	1	C2	15	Cz	15
		2	CP2	7	CPz	25
#7	Right	1	CP4	9	CP2	9
		2	C4	9	C4	11
#8	Left	1	CP5	5	CP3	7
		2	C5	5	C1	7
#9	Left	1	C3	9	C3	9
		2	C5	9	FCz	25
#10	Left	1	FCz	17	C1	7
		2	C3	17	FCz	17
#11	Left	1	C3	7	C3	7
		2	C5	11	FC1	15
#12	Left	1	C1	7	C1	7
		2	CP1	5	C3	17
#13	Right	1	C4	19	C4	19
		2	CP4	19	C6	7

Conversely, for the subject #6 the same spectral content (15 Hz) was significant for two neighbour EEG channels (i.e. C2 and Cz). Two possible trends were summarized in subject #7: first and second features similar from the spectral point of view (9 Hz) and topographical point of view, respectively. The first feature selected by the expert user became the second in the guided feature selection, for the subject #10. Summarizing, all features were coherent with the rehabilitative principles in terms of both topographic and spectral characteristics.

Figure 11 shows, for each dataset, the classification performances obtained using features selected by the expert neurophysiologist (manual procedure) and by the no-skilled user supported by the semi-automatic method (guided procedure). No significant differences were found between two procedures ($p=0.13$).

For both procedures, classification performances, on average 0.70 manual procedure, 0.69 guided procedure, were not as good as those that would have been obtained applying a k-fold cross-validation approach to data collected in the same session (e.g. chapter 3).

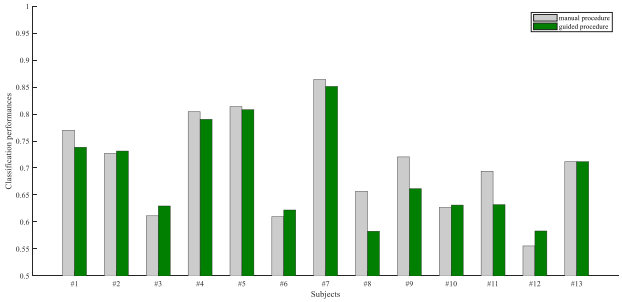

Figure 11 - For each subject (13 subacute stroke subjects) classification performance values obtained with features selected by manual (grey) and guided (green) procedures.

Using the second BCI training session could provide better results since the first training session could be considered a preliminary session where subjects become familiar with the experimental protocol and the kinesthetic imagination of the motor task.

However, when classification performances were higher than 0.7 the manual procedure seemed to outperform the guided procedure (not in statistical sense). Conversely when poor classification performances were reached the guided procedure returned better results. The subject #8 was the exception in term of both classification performance and

selected features. Indeed, basing on the EEG pattern visualization, it seemed that the pattern at 5 Hz conformed better to the expected pattern than that at 7 Hz, leading to better performances.

Discussion

Identifying the optimal control features is a milestone in rehabilitation protocols supported by BCI technology. In contrast to other fields of application where optimal cursor control is pursued, in a rehabilitation context the aim is to reinforce the appropriate sensorimotor activation in terms of both topographic and spectral characteristics. Therefore, the feature selection procedure requires knowledge coming from neurophysiology and rehabilitation principles as well as expertise in visualizing pattern of desynchronization in the form of statistical index matrices. The manual procedure is highly dependent on the operator and is currently restricted to researchers with experience in the BCI field. Therefore, the aim of GUIDER is twofold: first, to reduce the intra- and inter-operator variability of feature selection supporting the procedure also with a semiautomatic method but without giving up to neurophysiological principles that characterize the rehabilitation; second, to facilitate this procedure for therapists

without experience with BCIs. GUIDER could be, therefore, a (user-friendly) tool to support even non-expert users in the reproducible identification of control features, since it considers both neurophysiological and machine learning approaches.

However, in view of a wider employ of GUIDER, several limitations must be addressed in the near future, e.g. the implementation in MATLAB environment, which is subjected to licensing issue.

The results suggest that the features identified by the guided procedure are close to those chosen by experienced operators (manual procedure). Furthermore, both procedure's outputs are congruent with the physiological evidences. Moreover, in terms of classification performance, no statistical differences are found between the procedures. Hence, the choices of neurologists could be reproducible by a semiautomatic method that includes the operator and his neurophysiological knowledge in the procedure. Reproducibility is, indeed, a prerequisite for planning large multi-centric clinical trials, including a larger number of patients with several different operators, ensuring the comparability of BCI results among centres and thus increasing the generalizability of the results.

Main message

The introduction of GUIDER and its application in the BCI rehabilitation context suggest that it is feasible to support the professional end-users such as therapist/clinicians, who are not necessarily expert in BCI field, in the EEG feature selection yet according to evidence-based rehabilitation principles.

GUIDER employs a semiautomatic method and takes into account neurophysiological evidence and rehabilitation principles. Performances are as good as manual selection, and GUIDER allows reproducibility of the procedure. The latter is a prerequisite for planning large multi-centric clinical trials, including a larger number of patients with several different operators, ensuring the comparability of BCI results among centres and thus increasing the generalizability of the results.

Chapter 5
Adaptive learning in BCIs

Introduction

Brain state-dependent peripherical stimulation protocol induces significant plasticity of the damaged cortex in stroke patients, translating directly into improved functions [16]. The timing between the peripherical stimulation and the physiologically generated brain waves is the core of this approach to the motor rehabilitation post-stroke. Therefore, the early detection of the intended action (by MRCPs) in relation to the task onset is a key point.

In the last ten years, several methods for the MRCP detection have been developed based on the matched filter [45], the independent component analysis [46] , the locality preserving projections [47]. Recent studies have proposed the application of *manifold learning methods* to the MRCP detection. As demonstrated in [48], one of them, i.e. the Locality Sensitive Discriminant Analysis (LSDA), outperforms the method based on the locality preserving projection, resulting in more accurate and low-latency motor intention detection.

All proposed approaches analyse EEG data, recorded in the calibration session, to construct a transformation matrix later used to classify new EEG data. Therefore, there is neither adaptation after the initial training step nor exploitation of the new EEG data collected during the session.

Because of the continuously change in the brain activity occurring at the baseline but also during the task, current algorithms could become increasingly inefficient in applications if no-further calibration step is planned. Although adaptive learning has been successfully introduced in EEG [25], [49] and EMG [50] detection, at my knowledge there hasn't been any methodological transfer to MRCP detection.

This chapter proposes three adaptive learning methods based on LSDA [48]. The proposed algorithms constantly updated the model parameters of the MRCP detector to adapt to the subject's MRCP characteristics over time and use. This was achieved by exploiting EEG data collected in each task repetition and properly re-labelled basing on the force signal (recorded during the task): both past noise and MRCP observations were used to update the detector parameters.

Compare non-adaptive approach and three adaptive approaches, considering even the effect of the dataset size

used for the initial calibration, was the main aim of this work. Preliminarily, a study aimed to identify the best set of parameters to analyse EEG signals that minimizes the number of false positive detection was conducted.

Materials and Methods

Data Collection

Six healthy volunteers (males aged 20-28 years) with no previous history of neuromuscular disorders or lower limb pathology participated in the study. The data collection was held at Prof. J. Rothwell's Physiology and Pathophysiology of Human Motor Control Laboratory, Institute of Neurology, University College London (London, UK).

EEG, EMG and force data were simultaneously recorded: a trigger signal was used to synchronise the recordings. EEG data were collected from 64 electrodes assembled on an active-electrode cap (Brain Products GmbH, Germany) according to an extension of the 10-20 International System, amplified and sampled at 5000 Hz (per channel) by a commercial EEG system (BrainAmp, Brain Products GmbH, Germany). EEG recording were referenced at FCz and the ground electrode was positioned at Fpz. The skin was properly prepared and

impedance electrode-skin was adjusted to be below 5kΩ by filling the electrodes with an electrolytic gel. Surface EMG data were collected in bipolar fashion from a grid of 64 electrodes with 8mm inter-electrode distance (OT Bioelettronica, Turin, Italy) placed on the tibialis anterior muscle. The skin in the proximity of the muscle was shaved, lightly abraded and cleaned. EMG signals were band-pass filtered (10-500 Hz) and sampled at 2048 Hz (Quattrocento, OT Bioelettronica, Turin, Italy). The force signal was recorded from a force transducer mounted on a pedal, sampled at 2048 Hz and collected as auxiliary input by the amplifier used for the EMG signal collection.

The subject was seated in a comfortable chair and his right foot was fixed to a customized pedal. The experimental session started with the collection of the maximum voluntary contraction (MVC) force. Two MVC recordings were performed and the highest force value was used as reference. Each subject was instructed to perform four types of cue-based ankle dorsiflexion reaching the same target force (60% of MVC [51]). The types of dorsiflexion differed from each other for the movement speed: slow, medium, fast and ballistic i.e. 3s, 2s, 1s and as soon as possible in reaching the target force level. The visual cue gave the subject feedback on the speed of his

movements guiding the subject to perform the movement correctly (Figure 12). A preliminary training phase was also included to let the subject familiarize with the experimental procedure. For each task (e.g. ballistic task) the subject was trained to perform 25 isometric ankle dorsi-flexions. To reduce artefact contamination, the subject was invited to minimize muscular movements not involved in the task. Before each recording, EEG and EMG signals were visually inspected by the operator.

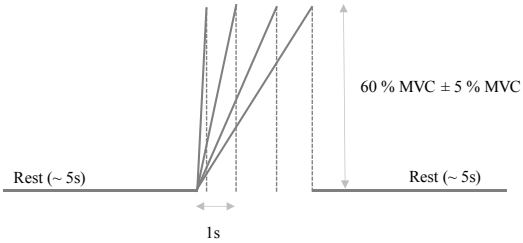

Figure 12 - Visual cue for the experimental task. After 5 seconds of rest, subject had to follow the force outline performing the ankle dorsiflexion and reaching the target force (60 ± 5 percentage of his maximum voluntary contraction, MVC) in ballistic fashion or in 1s (fast), 2s (medium), 3s (slow), before going back in the rest position. Each trial began when a cursor appeared in the left bottom side of the screen. The cursor moved on the line toward the right side at constant velocity. Its vertical position depended on the signal detected by the force transducer.

Data Analysis

EEG data were down sampled to 2048 Hz (i.e. the EMG data and force sampling frequency) and band-pass filtered from 0.05 to 2 Hz [52] with a 2nd order digital Butterworth filter in the forward and reverse direction. Because of the cortical region elicited by the ankle dorsiflexion only F3, Fz, F4, C3, Cz, C4, P3, Pz, P4 electrode positions were considered. To compensate for the resolution of scalp EEG, a large surface Laplacian spatial filter

was applied [45]. The EEG derivation, obtained according the expression

$$Cz^{rref} = Cz - \frac{(F3 + Fz + F4 + C3 + C4 + P3 + Pz + P4)}{8} \quad (5.1)$$

was segmented in trials (repetitions of the experimental task) accordingly to the cue-based paradigm. Trials containing instrumental artefacts, identified by the visual inspection, were removed from the analysis. On average, 23 trials were analysed for each subject. Force signal was low-pass filtered at 3 Hz and analysed to identify the movement onset. For each trial, the movement onset was detected when all values of the force signal in a window 0.2s long exceeded the threshold *th*, defined as $th = \mu + h \times \sigma$ (mean μ and standard deviation σ of the force signal in a window 1s long of the rest phase, h=3) and validated by visual inspection.

LSDA-based MRCP detector

LSDA [53] is a discriminant manifold learning method, useful when there is no sufficient training samples. In the latter cases, local structure is generally more important than global structure for discriminant analysis. By discovering the local manifold structure, LSDA finds the projection which maximizes the margin between data points from different classes at each local

area. Specifically, the data points are mapped into a subspace in which the nearby points with the same label are close to each other while the nearby points with different labels are far apart. The found linear transformation matrix (to map the high-dimensional data in a low-feature space) preservers the local neighbourhood information as well as the global discriminant information of the data.

Figure 13 shows the LSDA-based MRCP detection pipeline.

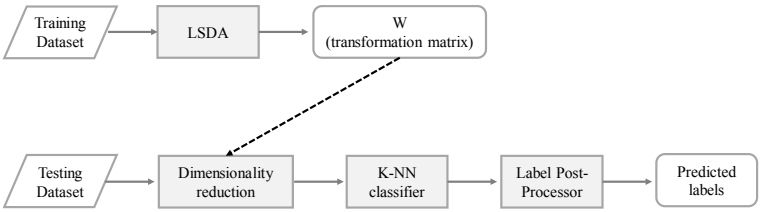

Figure 13 - The LSDA-based MRCP detection pipeline. *Upper panel* Training step: Transformation matrix (W) was computed applying LSDA algorithm to the training dataset. *Lower panel* Testing step: After the dimensionality reduction ($Testing\ Projection = W' \times Testing\ Dataset$), a k-nearest neighbors (k-NN) classifier returned the predicted labels, finally post-processed.

EEG signals were segmented in two classes: MRCP signal intervals and noise signal intervals.

In the segmentation process the following parameters were considered:

- duration of the segmentation time window
- first/last window labelled as MRCP (respect to the force onset)
- first/last window labelled as Noise (respect to the force onset)
- time window shift for MRCP training dataset
- time window shift for Noise training dataset
- time window shift for testing dataset
- k parameter of the nearest neighbors classifier.

EEG data were then split in two parts: one part used for the training step (training dataset) and the other used for the testing step (testing dataset). EEG segmented data belonging to the training dataset were the input of the LSDA algorithm. The transformation matrix W, found applying LSDA algorithm (parameters setting β=0.1 and k= 10) to the training dataset (Figure 13 upper panel), was multiplied by the testing dataset to reduce its dimensionality (from the initial feature space

dimension to 30, algorithm default value). Testing projections were classified using a k-nearest neighbors classifier [48]. The predicted label vector was post-processed by a shifting window 0.3s long. If the algorithm had classified as MRCPs at least two-thirds of the shifting window considered, an MRCP was detected.

To assess the performance of the MRCP detection pipeline two indices were computed,

- True Detection Rate (TDR), ratio of the number of task repetitions correctly detected to the total number of performed repetitions. More specifically, the true detection index (numerator of the TDR formula) was increased if the latency of the MRCP detection was in the interval [-0.8s 0.8s] respect to the onset detected by the force transducer. After MRCP detection, the classification was suspended for 3s (congruously with the duration of the MRCP evolution): in the associative-BCI at that time the nerve is stimulated and no further action is required from the classifier;

- False Positive per minute, FP/min, number of noise observations predicted as MRCPs in one minute long recording. As in TDR, after an MRCP had been detected

(even if a false positive) classification was suspended for 3 seconds.

Parameter optimization study

To investigate the befitting set of parameters that discriminated MRCP and Noise windows, preliminary tests were performed using the LSDA-based MRCP detector. All possible combinations of the parameter values were tested according to the procedure reported in the previous section and, for each subject and for each combination, performance indices were computed and analysed. In Table 3, for each parameter the set of admissible values tested. For the preliminary study, thirty percent of trials were used for the training step [48], the other part for the testing.

For each parameter set, the average performance value (TDR, FP/minute) across subjects was estimated and plotted on the Receiver Operating Characteristic space [35]. The point (one for each parameter setting) that minimized the FP/minute index, holding TDR over 70%, has been considered the point corresponding to the best set of parameters to discriminate MRCP and noise. The resulting set of parameters was then used for the comparison between non-adaptive algorithm and adaptive-algorithms.

Table 3 - Parameters and corresponding values tested in the MRCP detection model

Parameters	Tested values				
duration of the segmentation time window (s)	1.5	2.0 [48]	2.5	3	3.5
starting point of the first window labelled as MRCP respect to the force onset (s)	-3	-2.5	-2 [48]		
ending point of the last window labelled as MRCP respect to the force onset (s)	0.5				
Starting and ending point of the windows labelled as Noise respect to the force onset (s)			[-5 -2.5] U [1.5 5]		
time window shift for MRCP training dataset (s)	0.05 [48]	0.1			
time window shift for noise training dataset (s)	0.05 [48]	0.1			
time window shift for testing dataset (s)	0.05 [48]	0.1			
k parameter of the nearest neighbors classifier	1	2	3	4	5

Adaptive algorithms for MRCP detection

Three methods to adapt the model parameters of the MRCP detector were proposed and compared with no-adaptive approach. All methods are based on the LSDA, successfully used in [48] to detect MRCPs. All algorithms were trained with the same number of trials. While the non-adaptive algorithm (LSDA) did not change its parameters in time, the adaptive

methods modified their parameters repetition by repetition (trial by trial). The proposed scheme tried to simulate what happens in the online experimental protocol (cue-based). Once each task repetition had performed, EEG signal collected was segmented (according to the training dataset segmentation parameters) and properly relabelled based on the onset information collected from the force transducer. Both new observations (MRCPs and noise) were the input for the adaptive methods. All adaptive algorithms received the same new samples as input. The adaptive methods proposed are

- Locality Sensitive Discriminant Analysis followed by the Incremental updating of Linear Discriminant Analysis (LDSA + iLDA), Figure 14 upper panel; the linear transformation matrix (W) was computed one time, applied to the testing dataset to obtain testing projections. The latter were the input for the incremental Linear Discriminant Analysis [54] that updated its parameters every time new samples had been collected;

- Incremental updating of Locality Sensitive Discriminant Analysis (iLSDA), Figure 14 middle panel; every time new samples had been collected, the linear transformation

matrix (W) was re-computed and applied to new testing data;

- Incremental updating of Locality Sensitive Discriminant Analysis followed by the Linear Discriminant Analysis (iLSDA+LDA), Figure 14 lower panel; every time new samples had been collected the linear transformation matrix (W) was re-computed and applied to the new testing data, whose dimensionality was further reduced by the LDA algorithm.

Classification, post-processing and performance assessment have been consistent with those used in the LSDA-based MCRP detector (Figure 13).

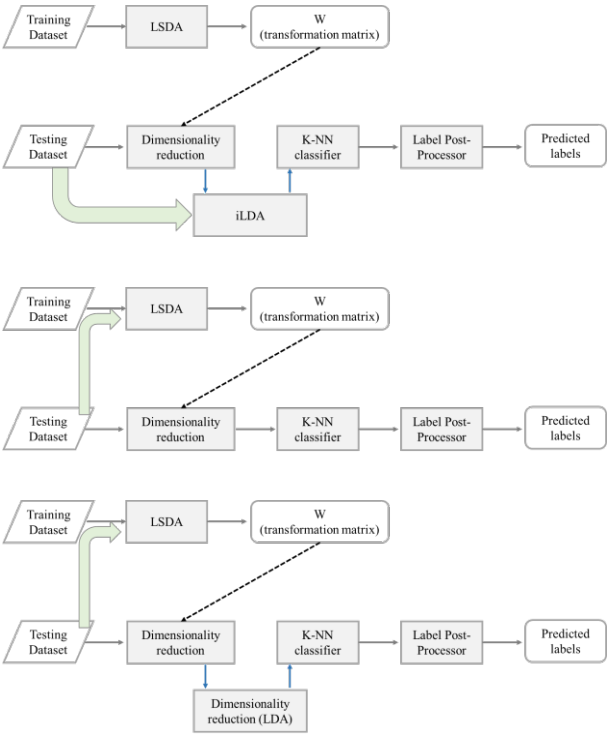

Figure 14 - Adaptive algorithm flowcharts. (*Upper panel*) LSDA followed by the incremental updating of the linear discriminant analysis (LSDA + iLDA), every time new EEG samples are collected, they update the parameters of the iLDA algorithm. (*Middle panel*) incremental LSDA (iLSDA), every time new EEG samples are collected, the linear transformation matrix (W) is re-computed and applied to new testing data. (*Lower panel*) incremental LSDA followed by the linear discriminant analysis (iLSDA+LDA), every time new samples are collected the linear transformation matrix (W) is re-computed and applied to the new testing data, which dimensionality is further reduced by LDA algorithm. For each panel, training data is used to compute the transformation

matrix by means the LSDA algorithm. Testing data are multiplied by the transformation matrix (W) to obtained the testing projections. The k-NN classifier and the label post-processor work as in the basic LSDA (Figure 13). All algorithms returned the predicted labels which were post-processed to compute performance indices.

MRCP detection algorithm comparison

For each method (non-adaptive LSDA and adaptive-algorithms) the whole procedure (Figures 13 and 14) was applied nine times to assess the effect of the initial training dataset size, from 10% to 90% (10% step) of the number of repetitions available for each subject. For each subject, classifier and training dataset size, two performance indices were computed: True Detection Rate (TDR) and False positive per minute (FP/min).

To investigate the performance of the LSDA algorithm as function of the percentage of repetitions (trials) used for the initial training, performance indices, True Detection Rate and False Positive per minute, were analysed by the repeated measure one-way analysis of variance (ANOVA). The Tukey HSD post hoc analysis was applied to assess pairwise differences. The threshold for statistical significance was set to $p<0.05$. All results are presented as mean ± SE (standard error).

Although it would have been very interesting to analyse the results obtained by means the repeated measures two-way ANOVA to investigate differences among algorithms and training dataset size and their interaction, the violation of the main hypotheses and the dimension of the sample (6 subjects) did not allow to apply the statistical design. Tables were used to compare the results. For each subject we identified the best classifier as the one that achieved good performance (high TDR and low FP/min) in most of the evaluated conditions.

For the best classifier (one for each subject) the median value (and the inter-quartile range, IQR) of the latency between the MRCP and the movement onset (detected from the force transducer) was computed. Negative (positive) values corresponded to MRCPs detected before (after) the real movement onset. Since all latencies have been referred to the movement onset, eventually positive latencies (MRCPs detected after the movement onset) would have affected the average value, used as main measure, resulting, therefore, in values very close to movement onset (0s) but not representative of the latency distribution.

Additionally, for the best classifiers the time required by the algorithm to update the parameters and perform one

classification, called running time, was computed and presented as mean ± standard deviation across trials. For conciseness, latency and running time were reported for each algorithm and subject only in the case of thirty percent of trials used for the initial training of the classifier.

Results

Results obtained in ballistic task are reported in this thesis. The following parameter values resulted the best set (according to the criterion defined in the paragraph Materials and Methods) to correctly detect MRCPs and reduce false positive detection: duration of the segmentation time window 2.5s, first and last time point labelled as MRCP respect to the force onset [-2.5 0.5]s, time window shift for MRCPs training dataset 0.05s, time window shift for noise training dataset 0.05s, time window shift for testing dataset 0.05s, k parameter of the nearest neighbors classifier, 2.

Figure 15 shows the performance indices, True Detection Rate and false detection per minute, of the LSDA algorithm (no-adaptive algorithm) as a function of the percentage of trials used to train the classifier. The repeated measures ANOVA did not reveal a significant effect of the percentage of trial factor on the true detection rate index ($F=1.70$, $p=0.13$). The same

statistical design revealed a significant effect of the percentage of trial factor on the false positive per minute index (F=3.74, p=0.002). For the latter the post-hoc test pointed out statistically significant differences between the classifier trained from the 10% of the dataset and those trained from larger dataset.

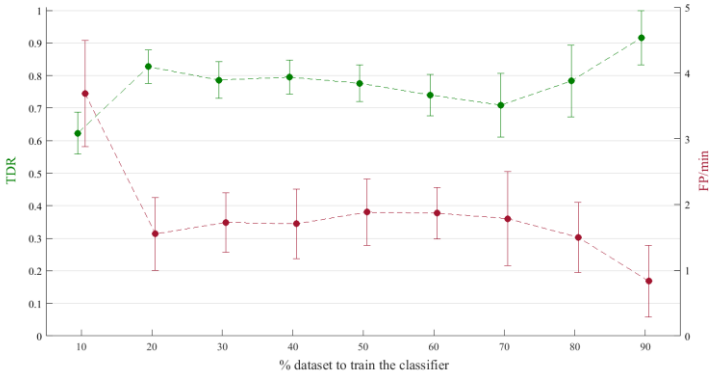

Figure 15 - True detection rate, TDR, *(Left axis*) and False Positive per minute, FP/minute, (*Right axis*), presented as mean ± SE (standard error, 6 subjects), as a function of the percentage of EEG data used for the initial training of the algorithm LSDA, locality sensitive discriminant analysis.

Although not confirmed by the statistical approach, the TDR index highlighted a similar trend: train the classifier with more samples (trials, i.e. repetitions of the task) increases the performance of the model, i.e. increase the ability to correctly

identify MRCP events (increasing in TDR) and to prevent false detection (decreasing in FP per minute).

Results, obtained applying the non-adaptive algorithm (LSDA) and considering the same amount of EEG data of that considered by Lin et al. in [48], matched those in [48] for the executed task (0.82 ± 0.14). Specifically, thirty percent of data used by Lin for the training of the classifier were equivalent to the forty percent of data used in this study. Even though subjects performed the ankle dorsiflexion as in this study, there are many differences among the studies: different experimental protocol, the number of task repetitions (fifty in [48] and at most twenty-five in our protocol) and the set of parameters used in MRCP detection. Moreover, they applied a 3-fold cross-validation approach that we could not use because the time sequence among trials is a basic requirement to explore the adaptive algorithms.

The high value of the standard error in both true detection rate and false positive per minute indices confirmed existing differences among subjects. Moreover, since at most twenty-five trials were available for each subject and since to test the adaptive algorithms we needed many trials, we decided to consider all trials available: no trials were discarded. The visual

inspection highlighted differences among trials (e.g. above all trials in ending part of the recording). Failures in the detection of those trials or detections too early or too late respect to the movement onset put down the performance of the classifier (Figure 16) and, therefore, the average across subjects (e.g. TDR at 70% in Figure 15).

Adaptive classifiers were developed to deal with EEG non-stationarity in order to track changes in EEG properties over time [25]. The adaptive algorithms proposed, implemented and tested are based on the LSDA algorithm proposed by Lin et al. in [48]. Tables 4-9 report the results, in terms of true detection rate and false positive per minute indices, for each subject and each dataset used for the initial training of the classifier with the best performing classifier typed in bold. While LSDA + LDA, iLSDA and iLSDA+LDA adapted the model parameters time by time (trials by trials), LSDA is the basic classifier as proposed in [48]. For each subject, the best classifier was identified by means the global score (sum of that in each performance index) achieved by each algorithm.

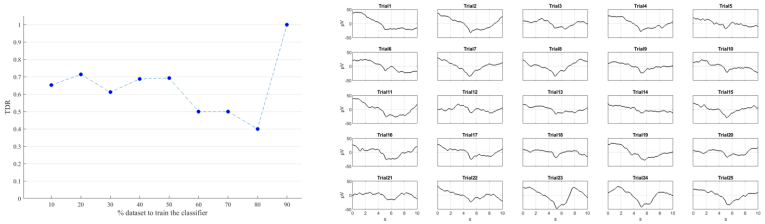

Figure 16 - *(Left Panel)* True detection rate, TDR, computed for the subject S01 and presented as a function of the percentage of EEG data used for the initial training of the algorithm LSDA, locality sensitive discriminant analysis. (Right Panel) Amplitude (μV) of the movement-related cortical potential (MRCP) as function of time (s) for each trial (25 trials). Train the model from eighty percent of trials (20 trials) and test by the last five trials has resulted in a minimum of the TDR curve (Left panel, TDR=0.4). Last five trials (e.g. trials 23 and 24) showed features different from the previous trials: they were identified 1.2s before the movement onset and, because of the constraints defined for the specific application, their detection did not increase the count of the true detection to eventually compute the true detection rate.

For the subject S01 (Table 4), detecting MRCPs by means the LSDA classifier did not return high performance in terms of true detections (TDR= 0.64 on average). As expected, use 90% of trials to train the classifier showed the best performance (TDR=1.00, FP/min =0.0). About TDR index, the adaptive algorithm iLSDA outperformed the no-adaptive LSDA: no effect of the initial training set size was observed.

Table 4 - Performance indices, True Detection Rate, TDR, and False Positive per minute, FP/min, for subject S01. Indices were computed for each percentage of EEG data used for the initial training of the algorithms. Algorithms: locality sensitive discriminant analysis (LSDA), LSDA followed by the incremental updating of the linear discriminant analysis (LSDA + iLDA), incremental LSDA (iLSDA), incremental LSDA followed by the linear discriminant analysis (iLSDA+LDA). For each performance index and percentage of the training set for the initial training of each algorithm, the best classifiers are typed in bold. The score achieved by each classifier, for each performance index, is reported in the last row of the table.

	LSDA		**LSDA + iLDA**		**iLSDA**		**iLSDA+LDA**	
	TDR	**FP/min**	**TDR**	**FP/min**	**TDR**	**FP/min**	**TDR**	**FP/min**
10%	0.65	2.1	0.70	3.7	**0.78**	**1.3**	0.65	3.7
20%	0.71	**1.4**	0.57	3.1	**0.76**	**1.4**	0.67	3.7
30%	0.61	**1.3**	0.67	3.3	**0.78**	**1.3**	0.72	3.3
40%	0.69	**1.1**	**0.88**	3.8	0.81	1.5	0.81	3.4
50%	0.69	**1.4**	0.69	3.2	**0.77**	1.9	**0.77**	3.2
60%	0.50	2.4	**0.70**	2.4	**0.70**	**1.8**	**0.70**	3.0
70%	0.50	**1.5**	**0.75**	3.0	0.63	2.3	0.63	3.0
80%	0.40	**1.2**	**0.80**	3.6	0.60	2.4	0.40	2.4
90%	**1.00**	**0.0**	0.67	**0.0**	**1.00**	**0.0**	0.33	**0.0**
	1/9	7/9	4/9	1/9	6/9	5/9	2/9	1/9

Conversely, similar performance has been reached in terms of FP per minute. LSDA and iLSDA reached same performance when ninety percent of trials had been used to train the classifier: perhaps just two trials were not enough to show and exploit the adaptive strategy of the iLSDA. Nevertheless, the iLSDA algorithm achieved good performance (TDR=0.78, FP/min=1.3) ever since the model had been trained from three trials (continuous recording long 30 seconds). The same effect illustrated in Figure 15 emerged and impacted also on adaptive algorithms: the early detection put down classifier performance.

For the subject S02 (Table 5), detecting MRCPs by means the LSDA classifier resulted in good performance (TDR= 0.9, FP/min=1.5, on average) as well as by means the adaptive algorithms. Nevertheless, for equal performance (TDR= 0.95, FP/min=1.1), the LSDA algorithm needed seven trials (continuous recording long 1 minute and 10 seconds), while the adaptive algorithm (e.g. iLSDA) just two trials (continuous recording long 20 seconds) to train the model. No differences were found among adaptive algorithms.

Table 5 - Performance indices, True Detection Rate, TDR, and False Positive per minute, FP/min, for subject S02. Indices were computed for each percentage of EEG data used for the initial training of the algorithms. Algorithms: locality sensitive discriminant analysis (LSDA), LSDA followed by the incremental updating of the linear discriminant analysis (LSDA + iLDA), incremental LSDA (iLSDA), incremental LSDA followed by the linear discriminant analysis (iLSDA+LDA). For each performance index and percentage of the training set for the initial training of each algorithm, the best classifiers are typed in bold. The score achieved by each classifier, for each performance index, is reported in the last row of the table.

	LSDA		**LSDA + iLDA**		**iLSDA**		**iLSDA+LDA**	
	TDR	**FP/min**	**TDR**	**FP/min**	**TDR**	**FP/min**	**TDR**	**FP/min**
10%	0.91	2.2	0.91	1.9	**0.95**	**1.1**	0.91	2.2
20%	0.89	**1.0**	**0.95**	1.6	**0.95**	1.3	**0.95**	2.2
30%	**0.94**	**1.1**	**0.94**	2.1	**0.94**	1.4	**0.94**	2.1
40%	0.86	**0.4**	**0.93**	1.7	**0.93**	1.3	**0.93**	1.3
50%	0.83	**0.5**	**0.92**	1.5	**0.92**	1.5	**0.92**	1.0
60%	0.80	**1.2**	**0.90**	1.8	**0.90**	1.8	**0.90**	**1.2**
70%	**0.86**	1.7	**0.86**	**0.0**	**0.86**	1.7	**0.86**	0.9
80%	**1.00**	2.4	**1.00**	**1.2**	**1.00**	2.4	**1.00**	**1.2**
90%	**1.00**	**3.0**	**1.00**	**3.0**	**1.00**	**3.0**	**1.00**	**3.0**
	4/9	6/9	8/9	3/9	9/9	2/9	8/9	3/9

For the subject S03 (Table 6), the LSDA+iLDA algorithm outperformed the no-adaptive algorithm. Although train the LSDA model with five trials (20% dataset size) resulted in good classification performance (TDR= 0.95, FP/min=0.6), similar performance had been achieved by the LSDA+iLDA algorithm using two trials (TDR= 0.91, FP/min=1.4) for the initial training of the classifier. Train the whole model, trial by trial, (iLSDA algorithm strategy) seemed to be effective in the reduction of false positive per minute. As reported for the subject S01, the constraints for the latency of the MRCP detection (fixed to increase the count of the true detections) put down the performance for all algorithms when the models had been trained with ninety percent of data.

For the subject S04 (Table 7), the iLSDA algorithm outperformed the no-adaptive algorithm in terms of TDR and the same approach followed by the linear discriminant analysis (iLSDA+LDA) resulted in optimal False Positive per minute index. No differences were found among classifiers when the model had been trained with more than fifteen trials (70% dataset size). Good results could be reached training the model with 2 trials (10% dataset size) and applying the adaptive strategy.

Table 6 - Performance indices, True Detection Rate, TDR, and False Positive per minute, FP/min, for subject S03. Indices were computed for each percentage of EEG data used for the initial training of the algorithms. Algorithms: locality sensitive discriminant analysis (LSDA), LSDA followed by the incremental updating of the linear discriminant analysis (LSDA + iLDA), incremental LSDA (iLSDA), incremental LSDA followed by the linear discriminant analysis (iLSDA+LDA). For each performance index and percentage of the training set for the initial training of each algorithm, the best classifiers are typed in bold. The score achieved by each classifier, for each performance index, is reported in the last row of the table.

	LSDA		**LSDA + iLDA**		**iLSDA**		**iLSDA+LDA**	
	TDR	**FP/min**	**TDR**	**FP/min**	**TDR**	**FP/min**	**TDR**	**FP/min**
10%	0.59	5.7	**0.91**	1.4	0.82	**0.8**	0.73	3.3
20%	**0.95**	0.6	**0.95**	0.6	0.89	**0.3**	0.79	2.5
30%	0.88	1.4	**0.94**	**0.4**	0.88	**0.4**	0.76	2.8
40%	**0.93**	1.7	**0.93**	**0.4**	0.86	**0.4**	0.71	2.6
50%	**1.00**	1.5	0.92	1.0	0.83	**0.5**	0.67	2.5
60%	**0.90**	1.2	**0.90**	**0.0**	0.80	0.6	0.60	2.4
70%	**0.86**	**0.0**	**0.86**	**0.0**	0.71	**0.0**	0.43	1.7
80%	**0.80**	**0.0**	**0.80**	**0.0**	0.60	**0.0**	0.20	**0.0**
90%	**0.50**	**0.0**	**0.50**	**0.0**	**0.50**	**0.0**	**0.50**	**0.0**
	7/9	3/9	8/9	6/9	1/9	8/9	1/9	2/9

Table 7 - Performance indices, True Detection Rate, TDR, and False Positive per minute, FP/min, for subject S04. Indices were computed for each percentage of EEG data used for the initial training of the algorithms. Algorithms: locality sensitive discriminant analysis (LSDA), LSDA followed by the incremental updating of the linear discriminant analysis (LSDA + iLDA), incremental LSDA (iLSDA), incremental LSDA followed by the linear discriminant analysis (iLSDA+LDA). For each performance index and percentage of the training set for the initial training of each algorithm, the best classifiers are typed in bold. The score achieved by each classifier, for each performance index, is reported in the last row of the table.

	LSDA		**LSDA + iLDA**		**iLSDA**		**iLSDA+LDA**	
	TDR	**FP/min**	**TDR**	**FP/min**	**TDR**	**FP/min**	**TDR**	**FP/min**
10%	0.60	1.8	**0.80**	1.5	**0.80**	0.9	**0.80**	**0.6**
20%	**0.83**	**0.3**	0.72	1.0	**0.83**	0.7	0.78	**0.3**
30%	**0.87**	0.4	0.67	1.6	**0.87**	0.8	0.80	**0.0**
40%	**0.92**	0.5	0.77	0.9	**0.92**	0.9	**0.92**	**0.0**
50%	0.82	1.1	0.73	1.6	**0.91**	1.1	**0.91**	**0.0**
60%	**0.89**	0.7	0.67	2.0	**0.89**	0.7	**0.89**	**0.0**
70%	**1.00**	**0.0**	0.86	**0.0**	**1.00**	**0.0**	**1.00**	**0.0**
80%	**1.00**	**0.0**	1.00	**0.0**	**1.00**	**0.0**	**1.00**	**0.0**
90%	**1.00**	**0.0**	1.00	**0.0**	**1.00**	**0.0**	**1.00**	**0.0**
	7/9	4/9	1/9	3/9	9/9	3/9	7/9	9/9

For the subject S05 (Table 8), the iLSDA+LDA algorithm outperformed the no-adaptive algorithm in terms of TDR (0.86 vs 0.71 on average), excepted for the training step with four trials (20% dataset size). Conversely, no differences were found in terms of False positive per minute among algorithms (except the best one in TDR). Training the model with two trials (10% dataset size) and applying the adaptive strategy of iLSDA or iLSDA+LDA allowed to achieve better results than those obtained not considering any adaptation (TDR=0.44, FP/min=6.3).

For the subject S06 (Table 9), the LSDA+iLDA algorithm improved performance in terms of both true detection rate and false positive per minute. Applying the adaptive strategy seemed to be resolutive in both MRCP detection and reduction of samples required for the initial training of the classifier. All classifiers reached the same performance training the models with most of EEG data (over 80% dataset size).

Table 8 - Performance indices, True Detection Rate, TDR, and False Positive per minute, FP/min, for subject S05. Indices were computed for each percentage of EEG data used for the initial training of the algorithms. Algorithms: locality sensitive discriminant analysis (LSDA), LSDA followed by the incremental updating of the linear discriminant analysis (LSDA + iLDA), incremental LSDA (iLSDA), incremental LSDA followed by the linear discriminant analysis (iLSDA+LDA). For each performance index and percentage of the training set for the initial training of each algorithm, the best classifiers are typed in bold. The score achieved by each classifier, for each performance index, is reported in the last row of the table.

	LSDA		**LSDA + iLDA**		**iLSDA**		**iLSDA+LDA**	
	TDR	**FP/min**	**TDR**	**FP/min**	**TDR**	**FP/min**	**TDR**	**FP/min**
10%	0.44	6.3	0.72	**2.0**	**0.83**	2.7	**0.83**	2.7
20%	**0.94**	**1.9**	0.81	2.3	0.88	2.6	0.81	2.6
30%	0.79	3.0	0.79	**2.1**	**0.86**	2.6	**0.86**	2.6
40%	0.75	3.5	0.83	3.0	0.83	**2.5**	**0.92**	3.0
50%	0.70	3.6	0.80	3.6	0.80	**3.0**	**0.90**	3.6
60%	0.63	**3.0**	**0.88**	3.8	0.75	**3.0**	**0.88**	3.8
70%	0.67	3.0	**0.83**	**2.0**	0.67	3.0	**0.83**	4.0
80%	0.50	**3.0**	0.50	**3.0**	0.50	**3.0**	**0.75**	4.5
90%	**1.00**	**0.0**	0.50	**0.0**	**1.00**	**0.0**	**1.00**	3.0
	2/9	4/9	2/9	5/9	3/9	5/9	8/9	0/9

Table 9 - Performance indices, True Detection Rate, TDR, and False Positive per minute, FP/min, for subject S06. Indices were computed for each percentage of EEG data used for the initial training of the algorithms. Algorithms: locality sensitive discriminant analysis (LSDA), LSDA followed by the incremental updating of the linear discriminant analysis (LSDA + iLDA), incremental LSDA (iLSDA), incremental LSDA followed by the linear discriminant analysis (iLSDA+LDA). For each performance index and percentage of the training set for the initial training of each algorithm, the best classifiers are typed in bold. The score achieved by each classifier, for each performance index, is reported in the last row of the table.

	LSDA		**LSDA + iLDA**		**iLSDA**		**iLSDA+LDA**	
	TDR	**FP/min**	**TDR**	**FP/min**	**TDR**	**FP/min**	**TDR**	**FP/min**
10%	0.54	4.0	**0.96**	**1.8**	0.83	3.0	0.88	2.5
20%	0.64	4.1	**0.95**	**1.6**	0.82	3.0	0.86	2.2
30%	0.63	3.2	**0.95**	**1.3**	0.79	2.8	0.84	1.9
40%	0.63	3.0	**1.00**	**1.5**	0.81	3.0	0.88	2.3
50%	0.62	3.2	**1.00**	**1.4**	0.85	2.8	0.92	2.3
60%	0.73	2.7	**0.91**	**1.6**	0.82	3.3	**0.91**	2.7
70%	0.38	4.5	**1.00**	**2.3**	0.75	4.5	0.88	3.8
80%	**1.00**	**2.4**	**1.00**	**2.4**	**1.00**	**2.4**	0.80	3.6
90%	**1.00**	**2.0**	**1.00**	**2.0**	**1.00**	**2.0**	**1.00**	**2.0**
	2/9	2/9	9/9	9/9	2/9	2/9	2/9	1/9

Since the latency in the MRCP detection is a key point in the rehabilitative protocol based on Hebbian theory, we needed to consider them as further performance index of the classifiers. For each subject the latency in MRCP detection for the LSDA algorithm and for the corresponding best classifier is reported in Table 10. In both LSDA and adaptive algorithms the MRCP detection has anticipated the real movement onset, confirming the possibility to detect in real-time the MRCP before the movement onset and, therefore, to apply the proposed algorithms in the context of the associative-BCI.

Table 11 presents for each subject and algorithm the mean runtime (across trials) to perform the parameter adaptation and the classification. As expected train again the whole model by means the LSDA (i.e. iLSDA) required more time than other algorithms.

Table 10 - Latency (expressed in seconds) in MRCP detection computed for each subject and for the LSDA algorithm (no-adaptive algorithm) and the best algorithm identified. Algorithms: locality sensitive discriminant analysis (LSDA), LSDA followed by the incremental updating of the linear discriminant analysis (LSDA + iLDA), incremental LSDA (iLSDA), incremental LSDA followed by the linear discriminant analysis (iLSDA+LDA). Results are presented as median value and inter-quartile range (IQR). Values below zero mean that the detections predate the movement onset (detected by the force transducer).

	LSDA		**LSDA + iLDA**		**iLSDA**		**iLSDA+LDA**	
	Median	**IQR**	**Median**	**IQR**	**Median**	**IQR**	**Median**	**IQR**
S01	-0.11	0.30			-0.16	0.35		
S02	-0.06	0.27	0.01	0.32	-0.16	0.35	-0.01	0.37
S03	-0.06	0.24	-0.03	0.30				
S04	-0.16	0.27					-0.06	0.15
S05	-0.21	0.42			-0.18	0.65	-0.18	0.70
S06	-0.21	0.52	-0.16	0.25				

Table 11 - Runtime (expressed in seconds) of each adaptive algorithm, presented as mean ± standard deviation (across trials). In the computation the time required for the initial training of the model based on LSDA were not considered. Algorithms: locality sensitive discriminant analysis (LSDA), LSDA followed by the incremental updating of the linear discriminant analysis (LSDA + iLDA), incremental LSDA (iLSDA), incremental LSDA followed by the linear discriminant analysis (iLSDA+LDA).

	LSDA	LSDA + iLDA	iLSDA	iLSDA+LDA
S01			0.67 ± 0.18	
S02		0.03 ± 0.01	0.41 ± 0.17	0.25 ± 0.09
S03		0.03 ± 0.01		
S04				0.20 ± 0.07
S05			0.26 ± 0.10	0.17 ± 0.07
S06		0.03 ± 0.00		

Discussion

To identify MRCPs with low-latency detection and good performances is essential in the context of BCIs based on the Hebbian principles. The approach proposed in this study aimed to overcome the limitations related to the physiological change occurring in time in the EEG signal, since these limitations impact on the use of BCI systems in rehabilitative protocols. Introduce adaptive learning methods in MRCP detection could represent a solution for the specific aim.

In this study we proposed, implemented and tested three adaptive algorithms. The latter are based on the LSDA algorithm proposed by Lin et al. in [48]. Considering the same validation approach (i.e. same number of trials used to train the detection model) we obtained in our dataset results (TDR ~80%) comparable to those obtained in [48] for LSDA approach. Including in the analysis all trials (no trials removal) reduced in some cases the performance of the algorithm, but, in view of an exploration of the efficacy of adaptive learning in MRCP detection, this could be considered an optimal scenario to test the performance of those approaches.

The application of adaptive strategies improved the performance of the LSDA algorithm. Considering each classifier

trained (for each subject) from ten percent of trials, we observed an improvement of performance indices, true detection rate ($TDR_{LSDA} = 0.62$, $TDR_{adaptive} = 0.87$, mean across subjects), and an effective reduction in false positive detection per minute ($FP/min_{LSDA} = 3.7, FP/min_{adaptive} = 1.5$, mean across subjects). Therefore, more MRCPs were properly detected and less noise samples were misclassified. Although no conclusive result could be provided about the best algorithm suitable for all subjects, the best single-subject algorithm filled the main requirements: high true detection rate, low false positive detection per minute, fast and low latency MRCP detection. All adapted algorithms, indeed, were able to detect MRCPs before the real movement onset, i.e. before any changes in EMG or force signal occurred. Moreover, all adaptive algorithms achieved good performances even though few samples had been used for the initial training step. In this way these approaches might remarkably reduce the time needed for the calibration of the system (20-30 seconds in adaptive algorithms vs more than 1 minute for the non-adaptive algorithm), directly impacting on patients in terms of preparation time before starting to use the BCI and increase of number of rehabilitative session.

Further studies are needed to increase the sample dimension, currently limited to six subjects, and the number of trials (repetitions of the task) recorded for each subject. An ongoing single-subject analysis on EEG data collected during two sessions (1 hour apart), each one consisted in thirty trials, is revealing that adaptive learning approach has the potential to be a promising approach to take on also changes occurring inter-sessions.

Finally, we decided to approach the investigation of adaptive learning methods in MRCP detection analysing EEG data collected during foot movements, since the effectiveness of the associative-BCI in the treatment of lower limb of stroke patients has already been validated in [16], but future works will be definitely targeted to transfer the methodology in protocols involving stroke patient upper limb.

Main message

The introduction of adaptive learning algorithms in the MRCP detection has the potential to reduce the calibration time of BCI system, directly impacting on the usability of the associative-BCI in post-stroke motor rehabilitation.

Chapter 6
Electromyographic features in hybrid BCIs

Introduction

Hybrid BCIs in post-stroke motor rehabilitation combine residual EMG activity with motor-related brain activation and provide a contingent reward which aims at re-establishing the link between the CNS and the periphery that is disrupted by the stroke [23].

The integration of residual EMG activity in BCI design for post-stroke motor rehabilitation requires some important clinical implications to be considered. Clear examples are the spasticity (i.e., an abnormal increment of the physiologic muscular resistance to passive/active movements) and the abnormal muscular synergies (i.e., abnormal functional recruitment of patterns of muscles) that are extremely common in post-stroke patients [55]. In this respect, the rehabilitative principle of promoting *good* plasticity and, thus, efficient functional recovery applies also to the muscular training/engagement possible operated by a hybrid BCI.

Several EMG features (e.g. amplitude of EMG signal of the target muscle) could be theoretically employed as well as several ways of combining EMG activity with brain derived activity to drive the BCI system can be hypothesized (e.g. a measure of cortico-muscular coherence). No consensus exists yet on these aspects and further studies are needed to define crucial aspects such as the “close-to-normal” EMG patterns to be reinforced or trained while discouraging those provoking spasticity and/or pathological synergies to eventually ensure a BCI mediated optimal re-establishment of brain-to-periphery connections.

Many studies dealt with the characterization of EMG activity after stroke in affected and/or unaffected upper limbs considering different task (i.e. reaching task, finger movements), different patients (i.e. chronic stroke patients) or different methods (i.e. motor unit decomposition [56], [57], [58], autoencoders [59], non-negative matrix factorization [60], [61], [62]). However, if the first method requires more complex set-up (i.e. high density EMG), for the last, literature provides contrasting results that do not allow to unequivocally clarify the effects of the injury and recovery mechanisms on the coordinated activity of muscle groups.

This chapter proposes a preliminary longitudinal study based on the analysis of the most frequently used features of EMG signals collected during simple tasks (hand opening and closing) accomplished by both affected and unaffected upper limbs in stroke patients before and after a rehabilitative intervention (i.e. BCI-supported MI-training). All patients, considered in this study, showed a clinical improvement after the rehabilitative intervention.

The main aim was to investigate if simple features (known to be modified by the stroke) provide information about the recovery mechanism post-stroke and, therefore, have to be considered in the designing of a new EMG signal feature related to *good* motor recovery after stroke, useful to control an hybrid BCI.

Materials and Methods

Data Collection

EMG signals from the flexor and extensor digitorum, long head of the biceps brachii, lateral head of the triceps brachii, lateral deltoid and pectoralis major muscles (Figure 17) of the affected and unaffected upper limbs were collected from twelve subacute stroke subjects according the procedure and the protocol in Appendix B.

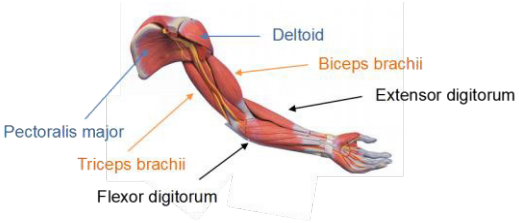

Figure 17 - Muscles recorded during the experimental protocol from both upper limbs (unaffected and affected).

Briefly, in both Pre- and Post- intervention sessions, subjects were instructed by the therapist to execute (or attempt) the hand opening and closing using their unaffected and affected upper limbs (all combinations recorded in separate runs). In each run, subjects were asked to perform 15 ±1 repetitions (trials) of the task. Each trial comprised 3 seconds of rest and

4 seconds of task (in 4s subjects had to start and complete the movement).

A set of specific functional scales was administered before and after the intervention. Three outcome measures (Table 12) were included in the clinical assessment: the arm section of the Fugl–Meyer Assessment (FMA), the upper limb section of the Medical Research Council scale for muscle strength (MRC) and the upper limb section of the MAS for spasticity. The same operator performed the clinical assessment in Pre- and Post-intervention session.

Table 12 - Demographic and clinical characteristics of stroke patients. For each patient sex (M, male; F, female), age (in years), time from event (in months), event description, affected hemisphere (R, right; L, left), clinical evaluations in term of Medical Research Council (MRC) Scale for muscle Strength, Modified Ashworth Scale (MAS) for spasticity, Fugl-Meyer Assessment (FMA) Scale, evaluated in Pre-intervention session (top row) and Post-intervention session (bottom row).

ID	Sex (M/F)	Age (years)	Event (months)	Event description	Hemisphere affected	MRC	MAS	FMA
#1	M	47	1	Subcortical ischemic	L	50 52	4 5	15 18
#2	M	62	1	Subcortical haemorrhagic	L	67 73	0 0	40 54
#3	M	65	1	Cortical ischemic	L	70 77	0 0	43 57
#4	F	71	1	Subcortical ischemic	R	76 69	0 0	59 62
#5	M	58	1	Subcortical ischemic	R	63 68	0 0	35 43
#6	F	50	1	Ischemic	R	43 69	0 1	8 45
#7	F	75	2	Subcortical ischemic	L	56 72	5 3	31 58
#8	F	62	2	Subcortical haemorrhagic	L	55 68	2 4	17 42
#9	F	82	2	Cortical ischemic	R	59 70	0 2	20 47
#10	M	58	3	Subcortical ischemic	L	60 62	6 8	29 32
#11	M	52	3	Subcortical ischemic	R	49 55	3 3	10 17
#12	M	76	4	Subcortical ischemic	R	51 52	0 0	10 13

NOTE: Medical Research Council (MRC) Scale for muscle strength, upper limbs, ranging from 0 (most affected) to 80 (least affected); Modified Ashworth Scale (MAS) for spasticity in the upper limb joints, ranging from 0 (least affected) to 24 (most affected); Fugl-Meyer Assessment (FMA) scale, upper limb section, ranging from 0 (most affected) to 66 (least affected).

Data Analysis

For each subject, the EMG signals collected during the execution of the experimental tasks (hand opening and closing) with

- the unaffected upper limb in Pre-intervention session, from unaffected upper limb muscles
- the affected upper limb in Pre-intervention session, from both upper limb muscles
- the affected upper limb in Post-intervention session, from both upper limb muscles

were analysed.

EMG signals were offline bipolarized, digitally high-pass filtered (20 Hz [63], cut-off frequency, second-order zero-lag Butterworth digital filter) and notch filtered to remove the power line interference (50 Hz). EMG recordings (only those contaminated from the electrocardiographic, ECG, signal) were pre-processed using the method proposed by Willingenburg et al. [64] to remove ECG contribute. For each dataset the procedure was validated by the operator, who had also visually inspected the EMG signals to identify signals corresponding to

missing contacts. Bad trials (in term of both task repetitions and muscles) were eliminated from the later analysis. Therefore, for each subject different number of trials (less than fifteen) and number of muscles were considered.

Time Domain Univariate Analysis

For each subject, session (Pre- and Post- intervention), task (opening and closing hand), upper limb (affected and unaffected) and muscle, the onset time of the muscle contraction has been computed for each trial (repetition of the task). As shown in [65], indeed, the delay of initiation of muscle contractions between the affected and unaffected upper limbs is a significant feature in stroke patients.

The method proposed by Solnik et al. [66], based on the combination of Teager-Kaiser energy operator and threshold algorithm [67], was applied (baseline window 1s long) and adjusted to match the dataset characteristics: baseline window was computed trials by trials and amplitude threshold was set to h=6 [68]. Procedure results have been validated by the operator visual inspection. Onset time values of forearm muscles (extensor and flexor digitorum) were analysed: subjects' upper limb placement and experimental task (that had

elicited the activation of both muscles for most of subjects) made reasonable the comparison.

For each task (hand opening/closing), muscle (extensor and flexor digitorum) and condition (unaffected upper limb in the Pre-intervention session, affected upper limb in both Pre- and Post-intervention sessions) the median of onset time values was chosen as the emblematic value of each distribution. Since the pathological condition would not have allowed subjects to perform the movement in the same fashion, outliers would have influence on the mean value. Single-subject and group analysis were conducted to investigate changes in the onset time value both as stroke (alterations between unaffected and affected muscle in Pre-intervention session) and as rehabilitative (recovery of the affected muscles between Pre-intervention and Post-intervention sessions) result.

Amplitude Domain Univariate Analysis

EMG signals were full-wave rectified and low-pass filtered (1 Hz cut-off frequency, second-order zero-lag Butterworth digital filter) to obtain the envelopes.

To extract amplitude indices to compare sessions (unaffected muscles in the Pre-intervention session, affected muscles in the

Pre-intervention session and affected muscles in the Post-intervention session) we needed to normalize EMG signals to a value obtained from a reference contraction. Since maximum voluntary contractions (MVCs) were not available, a submaximal voluntary contraction was computed for each muscle and subject according to the procedure described below:

- flexor digitorum muscle, submaximal voluntary contraction was computed analysing data collected from the unaffected upper limb flexor digitorum muscle during the hand closing task (flexor digitorum muscle is the agonist muscle in hand closing task);

- extensor digitorum muscle, submaximal voluntary contraction was computed analysing data collected from the unaffected upper limb extensor digitorum muscle during the hand opening task (extensor digitorum muscle is the agonist muscle in hand opening task);

For each trial the root-mean-square (RMS) value of the EMG signal (moving window 0.05 s long [69]) was computed. The 95° percentile of the intra- and inter-trial RMS values was considered as the reference value for the normalization step.

After normalizing the envelopes of forearm muscles by the submaximal voluntary contraction values, maximum activation level and baseline activation level were computed for each trial as, respectively, the 95° and 5° percentile of the normalized envelope.

Spatial Domain Univariate Analysis

To investigate if proximal muscles were involved in simple tasks (hand opening and closing), the results of the time domain univariate analysis were further post-processed. The percentage of trials (respect to the total number of trials analysed for each subject) in which activation had been detected was computed for each muscle.

To analyse results and compare them in the conditions of interest (task performed with the unaffected upper limb in Pre-intervention session, task performed with the affected upper limb in both Pre- and Post- intervention sessions) a spatio-condition representation was designed. For each task and subject, the representation included the number of activations of each muscle (x-axis) for each condition (y-axis). For each point (muscle-condition) a circle, diameter proportional to the number of activation written inside as percentage of the total

number of trials, was plotted. Colours were related to the upper limb segment to which muscles belong.

For the spatial analysis only five subjects were considered. The other subjects were removed from the analysis because there were no good quality signals available for all considered muscles and sessions.

Statistical Analysis

Statistical analysis was performed to investigate global characteristic of the experimental group. Since the group analysis might not provide statistical evidence because of the differences intra-group and the few patients who performed movements with the affected upper limb (in Pre-intervention session), single-subject analysis results were used to explain trend not statistically confirmed.

Onset time and activation level values were analysed to assess differences among the conditions: unaffected upper limb in Pre-intervention session, affected upper limb in Pre-intervention session and affected upper limb in Post-intervention session. Shapiro-Wilk test was applied to assess the normality of the data distribution. To investigate differences among the conditions as a function of the muscle (flexor digitorum and

extensor digitorum muscles), a repeated measures two-way analysis of variance (ANOVA) design was employed as statistical design. The Tukey HSD post hoc analysis was applied to assess pairwise differences. The threshold for statistical significance was set to $p<0.05$. Results are presented as mean ± SE (standard error).

Results

Time Domain Univariate Analysis

Figure 18 shows for each task (hand opening and closing) the onset time of the muscle contraction, presented as mean ± SE (across subjects), evaluated for unaffected and affected flexor and extensor digitorum muscles in the Pre-intervention session and for affected muscles in the Post-intervention session. Subjects with residual motor ability (muscular activation detectable by the applied algorithm, see section Time Domain Univariate Analysis in Materials and Methods paragraph) were considered for the group statistical analysis.

Shapiro-Wilk tests confirmed the possibility of analysing data using parametric statistical design (i.e. ANOVA). For the opening task (8 subjects), the repeated measures two-way ANOVA revealed a significant effect of both session-side

(F=3.765, p=0.049) and muscle (F= 9.532, p= 0.018) main factors and no significant interaction factor (F=3.661, p= 0.053). For the closing task (7 subjects), the repeated measures two-way ANOVA did not reveal a significant effect of either session-side main factor (F=1.459, p=0.271) or muscle (F= 0.020, p= 0.891) main factor and no significant interaction between the session-side and muscle factors (F=0.523, p= 0.605).

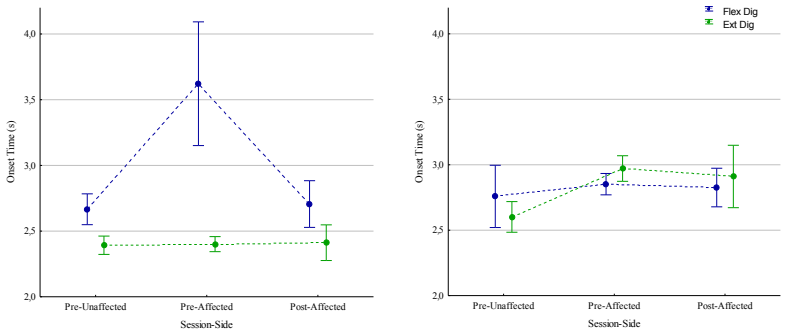

Figure 18 - Onset Time of the muscle contraction measured (in seconds) respect to the beginning of each repetition of the task. Results are presented as mean ± SE (standard error) across subjects and evaluated for each condition, unaffected upper limb muscles in Pre-intervention session (Pre-Unaffected), affected upper limb muscles in Pre-intervention session (Pre-Affected), affected upper limb muscles in Post-intervention session (Post-Affected) and for each muscle, flexor digitorum (Flex Dig, in blue) and extensor digitorum (Ext Dig, in green). Left panel: Hand opening. Right panel: Hand closing.

Results confirmed the findings in [65] about the delay initiation of muscular contraction between affected (Pre-intervention session) and unaffected (Pre-intervention session) upper limb muscles. In hand opening task, the post-hoc test pointed out the significant statistical difference existing in flexor digitorum muscle onset time (flexor digitorum muscle is a stabilizing muscle for the specific task) between the unaffected and the affected side ($p=0.04$). Moreover, following a similar approach to that proposed in [65], the onset time delay between affected and unaffected flexor digitorum muscle was resulted to be correlated (correlation coefficient= 0.64) with the level of impairment (MRC in Pre-intervention session).

In hand closing task there was a trend (not statistically supported) consistent with the findings in [65]: both agonist (flexor digitorum muscle) and stabilizing (extensor digitorum muscle) muscles of the affected side have been activated later than those of the unaffected side. Single-subject analysis (not reported in the thesis for conciseness) provides information to explain the statistical results: two subjects (subjects #7 and #8, seven in total) exhibited an opposite trend (respect to that expected result) in the comparison unaffected and affected side Pre-intervention. Further investigations including behavioural and clinical evaluations could clarify the relation

between the impairment and the delay in onset time of muscular contraction.

Moreover, the increasing trend of the onset time value in the comparison between unaffected and affected muscles (Pre-intervention) has been turned into a decreasing trend of the onset value when the comparison between Pre-intervention session affected muscles and Post-intervention session affected muscles was considered. More specifically, in hand opening task, Tukey post-hoc test pointed out ($p=0.05$) a statistically significant difference for the stabilizing muscle that not only anticipated its activation respect to the Pre-intervention session but reached also a value, on average, closer than that of the unaffected upper limb in the Pre-intervention session. The anticipation of the onset time in Post-intervention session respect to the Pre-intervention session for the stabilizing affected muscle, expressed in percentage respect to onset time in the Pre-intervention session, seemed to be correlated (coefficient of correlation 0.54) with the difference in clinical evaluations (i.e. MRC) assessed in the Pre-intervention and Post-intervention sessions.

The similar trend (anticipation respect to the affected condition Pre-intervention) was observed (even though not statistically

confirmed) in the hand closing task for both stabilizing and agonist muscles. Single-subject analysis revealed that subjects (i.e. #7 and #9), who showed a different trend between muscles, e.g. delayed onset time for stabilizing muscle and anticipated onset time for agonist muscle in the comparison Pre-Post intervention of the affected side, have been characterized by the similar clinical assessment in the Pre-intervention session, i.e. MRC evaluation equal to 56 (subject #7) and 59 (subject #9). Moreover, “small” clinical improvements coincided with no significant alteration of the onset time in the affected side muscles (subject #11, MRC scale assessment 49 in Pre- and 55 in Post- intervention sessions, FMA scale assessment 10 in Pre- and 17 in Post-intervention sessions).

The relation existing between flexor and extensor digitorum muscles was also investigated and confirmed by the significant main effect pointed out by the ANOVA results for the hand opening task: the activation of the extensor digitorum muscle (agonist muscle in the specific task) foreran the activation of the flexor digitorum (most affected by the stroke). The anticipation trend was consistent in all conditions evaluated, providing us general information about the characterization of the simple task considered. Single-subject analysis pointed out interesting considerations for four subjects. For subjects #9 e

#4 in post-intervention session the activation sequence, altered in the affected upper limb in the Pre-intervention session in term of simultaneous activation (#9) and pre-activation (#4) of the stabilizing respect to the agonist muscle) returned toward a sequence more similar to other subjects (i.e. agonist activation foreruns the stabilizing muscle activation). Moreover, for subjects #1 and #6, who in the first assessment (Pre-intervention session) did not show muscle activation, there was an improvement in term of muscles recruitment and proper timing sequence between extensor and flexor digitorum. While subject #6 ($MRC_{Post} - MRC_{Pre} = 26$) has activated extensor before the flexor muscle, subject #1 , who exhibited a lower improvement ($MRC_{Post} - MRC_{Pre} = 2$), has simultaneously activated agonist and stabilizing muscles.

In hand closing task no effect of the muscle factor was pointed out by the statistical analysis. Single-subject analysis revealed variability intra- and inter-subjects in term of both anticipation and delay of the stabilizing muscles respect to the agonist muscles.

Some useful information was provided from the analysis of the delay respect to the visual cue: even if therapists instructed subjects to perform the movement when the cursor crossed the

boundary between the black and the green space (3s after the start of each trial), the anticipation of the onset time respect to the cue was consistently observed in all conditions (for agonist muscles in both tasks). Two exceptions: subjects #1 and #12 in Post-intervention session started the muscle contraction after the cue.

Amplitude Domain Univariate Analysis

Figure 19 shows for each task (hand opening and closing) the maximum activation level, presented as mean ± SE (across subjects), evaluated for both unaffected and affected upper limb (flexor and extensor digitorum muscles) in the Pre-intervention session and for affected upper limb in the Post-intervention session.

Shapiro-Wilk tests confirmed the possibility of analysing data using parametric statistical design (i.e. ANOVA). For the opening task (10 subjects) repeated measures two-way ANOVA revealed significant effect for the session-side factor ($F=6.239$, $p=0.009$); muscle factor ($F=0.229$, $p=0.644$) and interaction factor ($F= 0.419$, $p=0.664$). For the closing task (11 subjects) repeated measures two-way ANOVA revealed a significant effect for the muscle factor ($F=5.627$, $p=0.039$); session-side

factor (F=0.859, p=0.439) and interaction factor (F= 2.449, p=0.112).

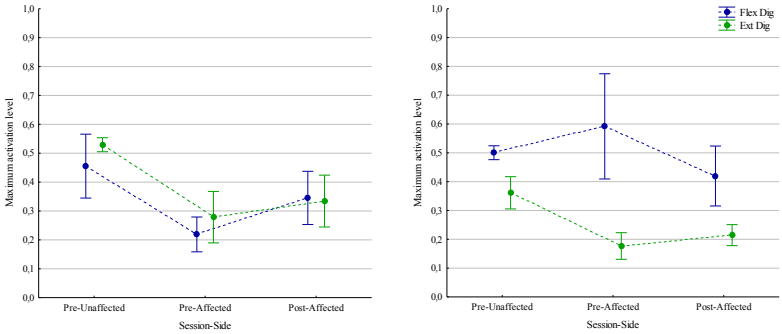

Figure 19 - Maximum activation level (normalized value, see Materials and Methods paragraph for the procedure), presented as mean ± SE (standard error) across subjects, evaluated for each condition, unaffected upper limb muscle in Pre-intervention session (Pre-Unaffected), affected upper limb muscle in Pre-intervention session (Pre-Affected), affected upper limb muscle in Post-intervention session (Post-Affected) and muscles, flexor digitorum (Flex Dig, in blue) and extensor digitorum (Ext Dig, in green). *Left panel*: Hand opening task. *Right panel*: Hand closing task.

In hand opening task Tukey post-hoc test pointed out significant statistical difference for both muscles between the unaffected and affected side in term of maximum activation level evaluated in Pre-intervention session, confirming, although in different task and muscles, the impact of stroke alterations on the maximum activation level found in [70].

The extensor digitorum muscle showed the same trend, even if not statistically supported, in the hand closing task. On the other hand, in the flexor digitorum muscle (agonist muscle for the specific task) the increasing average value of the maximum activation level (respect to the unaffected side condition) coincided also with an increasing value for the standard error than that observed in other session-side conditions and muscles.

After the rehabilitative intervention (post-intervention) the maximum activation level increased in the forearm muscles of the affected upper limb (except for the subject #12 for whom clinical evaluations confirmed a poor recovery in term of both MRC and FMA evaluations). Group heterogeneity did not allow to provide statistical proof of single-subject analysis results. In a similar fashion, the average activation level for stabilizing muscle increased in hand closing task. The large standard error in the affected flexor muscle after the intervention than that of the extensor muscle confirmed different behaviours in subjects for the flexor digitorum muscle. The significant main effect of the muscle factor in the hand closing task confirmed the higher contribute of flexor muscle in the hand closing than that of the extensor muscle. In the hand opening task no-significant

muscle factor effect suggested the similar contribute of agonist and stabilizing muscles in that task.

Figure 20 shows for each task (hand opening and closing) the baseline activation level, presented as mean ± SE (across subjects), evaluated for both unaffected and affected upper limb (flexor and extensor digitorum muscles) in the Pre-intervention session and for affected upper limb in the Post-intervention session.

In the opening task (10 subjects) as well as in the closing task (11 subjects) repeated measures two-way ANOVA did not reveal statistical differences: session-side factor ($F=1.746$, $p=0.203$, opening; $F=0.338$, $p=0.717$, closing), muscle factor ($F=4.145$, $p=0.072$, opening; $F=4.042$, $p=0.072$, closing) and interaction factor ($F=1.035$, $p=0.375$, opening; $F=2.166$, $p=0.141$, closing).

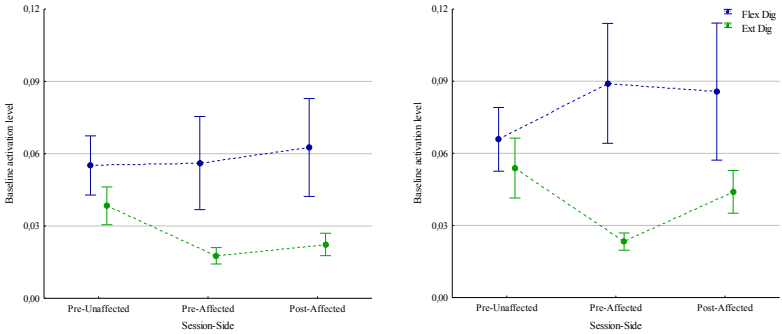

Figure 20 - Baseline activation level (normalized value, see Materials and Methods paragraph for the procedure), presented as mean ± SE (standard error) across subjects, evaluated for each condition, unaffected upper limb muscle in Pre-intervention session (Pre-Unaffected), affected upper limb muscle in Pre-intervention session (Pre-Affected), affected upper limb muscle in Post-intervention session (Post-Affected) and muscles, flexor digitorum (Flex Dig, in blue) and extensor digitorum (Ext Dig, in green). *Left panel*: Hand opening task. *Right panel*: Hand closing task.

Although statistical analysis did not reveal a statistical effect of the muscle factor: the baseline activation level is higher in flexor digitorum muscle than in extensor digitorum. Moreover, differences across subjects (proved by the larger standard error in flexor than in extensor muscles) did not suggest alterations related to the affected upper limb or condition before and/or after intervention.

On the other hand for extensor digitorum muscles, even if not strongly verify from the statistical point of view, the single-subject analysis revealed decreasing/increasing trends passing from un-affected limb to affected limb in Pre-intervention session and from Pre- to Post- intervention in the affected upper limb respectively (exception #8 and #12 in closing and #8 in opening).

Spatial Domain Univariate Analysis

Figures 21 and 22 show some results of the analysis in the spatial domain. Understanding if muscles different from forearm muscles were involved in the simple hand opening and closing task was the main goal of this analysis. Therefore, each representation (one for each subject and task) shows muscles recruited while the subject performed the task with the unaffected upper limb during the Pre-intervention session, the affected upper limb during Pre- and Post-intervention sessions. Both subjects (#5 and #11) are right-hemisphere lesioned, therefore, right and left were, respectively, the unaffected and affected upper limbs.

Both subjects exhibited activations of proximal muscles even during the task execution with the unaffected hand. More specifically, while subject #5 has recruited biceps brachii during

the hand closing and triceps brachii during the hand opening task, subject #11 has recruited in any case the biceps brachii. In the Pre-intervention session to execute the affected hand opening and closing tasks the subject #5 has activated flexor and extensor muscles of the affected upper limb as well as those of the unaffected upper limb. Rehabilitative intervention resulted in the reduction in number of activations of muscles of the unaffected limb during the affected limb movement.

Subject #11, different in term of clinical assessment from the subject #5, showed strong (in term of number of trials in which muscles have been activated) activation of the unaffected upper limb during the task performed with the affected upper limb. The map suggests the effectiveness of the rehabilitation in term of reduction of the unaffected muscle activations. Rehabilitation did not change the spatial distribution of muscles involved in the task executed with the affected limb: distal and proximal muscles have been activated also after the rehabilitative intervention.

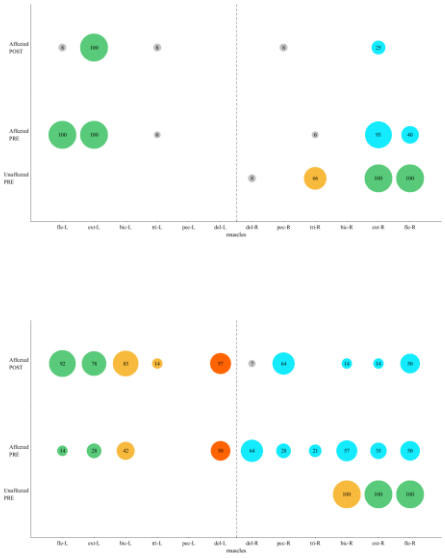

Figure 21 - Spatio-condition representation of the hand opening task. Number of activations, as percentage of the total number of repetitions, evaluated for the muscle reported on x-axis in the condition reported on y-axis. Three conditions have been considered (from bottom to top, movement executed with unaffected upper limb in Pre-intervention session, with affected upper limb in both Pre- and Post-intervention sessions). For each point (muscle-condition) the diameter of the circle is proportional to the number of activations in the circle. Colours correspond to the upper limb segment to which muscles belong (green forearm, yellow arm, red shoulder, light blue unaffected limb during task executed with the affected upper limb). *Upper panel* Subject #5. *Lower panel* Subject #11.

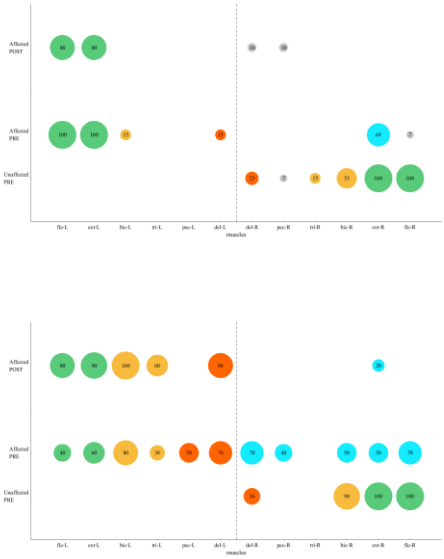

Figure 22 - Spatio-condition representation of the hand closing task. Number of activations, as percentage of the total number of repetitions, evaluated for the muscle reported on x-axis in the condition reported on y-axis. Three conditions have been considered (from bottom to top, movement executed with unaffected upper limb in Pre-intervention session, with affected upper limb in both Pre- and Post-intervention sessions). For each point (muscle-condition) the diameter of the circle is proportional to the number of activations in the circle. Colours correspond to the upper limb segment to which muscles belong (green forearm, yellow arm, red shoulder, light blue unaffected limb during task executed with the affected upper limb). *Upper panel* Subject #5. *Lower panel* Subject #11.

Discussion

Promoting motor function recovery is the main goal of post-stroke rehabilitation. Reinforcing voluntary contraction reflecting correct muscle activation and discouraging pathological synergies are the core of the EMG approach proposed by this work in the context of hybrid EEG-EMG BCIs. This preliminary study aimed to explore the meaning of the expression “correct muscle activation” to ultimately identify descriptors to include in the definition of the electromyographic feature reflecting the “good recovery”. In this view EMG data from subacute stroke subjects collected before and after the rehabilitative intervention in [9] were analysed to assess stroke alterations (difference in EMG pattern between unaffected and affected upper limb while performing simple movement i.e. hand opening and closing) and to characterize post-stroke recovery considering the difference in EMG pattern between affected upper limb before and after the rehabilitative intervention.

Stroke impacts on time and amplitude electromyographic features. Results presented in this thesis suggest that also simple tasks such as hand opening and closing are affected from changes caused by stroke. Specifically, stabilizing

muscles (i.e. flexor digitorum in hand opening task and extensor digitorum in hand closing task) were more affected by the injury than agonist muscles in terms of delay of the onset time of muscle contractions respect to that observed in unaffected side. Agonist and stabilizing muscle resulted impaired by stroke in terms of reduction of the maximum activation level in hand opening task confirming the difficulty that stroke survivors experience in extending fingers and thumb.

The anticipation of onset time of muscle contraction and the increasing value of the maximum activation level (comparing the affected muscles between Pre- and Post- rehabilitative intervention sessions) seem to be features of motor recovery (the latter already proved by clinical assessment). Further studies will be needed to assess if it is recovery or just inter-session variability. In addition, move towards the feature values of the unaffected hand highlights the open issue linked to the meaning of *good recovery* in terms of *likeness* with the unaffected hand of each stroke subject or with healthy subjects.

Stroke impacts on the muscles recruited to perform motor tasks too. Even if also in the unaffected hand movements proximal muscles seem to be enrolled to perform the task,

stroke subjects engage more muscles as well in the affected as in the unaffected upper limbs while performing movements with the affected hand. Discussion is currently open with expert neurophysiologists to understand if e.g. the reduction in activations of muscles from the unaffected side might be guessed a significant feature to monitor the recovery.

Current works are focused on the simultaneously analysis of more muscles, considering both time and amplitude features. Even if many couples of muscles (to better understand the meaning of pathological synergy) will be subjected to my investigation, I am focusing on flexor and extensor digitorum muscles, trying to overcome the actual shortcomings related to the definition of baseline for the onset time detector and the submaximal voluntary contraction.

To date differences among subjects, enrolled at different time from the stroke event and heterogeneous from the clinical point of view, as well as the lack availability of all muscles for all subjects did not lead to conclusive evidences.

Main message

Stroke impacts on the features of the electromyographic signals, altering performance in daily life activities. Consider both time and amplitude features in the designing of a new feature for an hybrid EEG-EMG BCI system could provide information about recovery. The simultaneous collection of signals from both distal and proximal muscles could highlight useful elements to discourage pathological synergies.

General Conclusion

Transfer BCIs to clinical realm requires making them more affordable, more efficient, and more usable. This PhD thesis proposed new algorithms and signal processing procedure to fulfil these requirements. Specifically, it introduced

- a new physiologically-driven approach to the pre-processing of BCI data that allows to reduce the number of EEG electrodes to collect (lower equipment cost, reduced setup up, less burden for therapist and patient),

- a new semiautomatic physiologically-driven method to support professional end-users, not necessarily expert in BCI field, in the EEG feature selection for SMRs-BCI training according to evidence-based rehabilitation principles (wider employment of the technology),

- adaptive learning algorithms in MRCPs detection that allow to reduce the calibration time (less burden for the patient, more treatment sessions),

- new elements to design a new control feature for the hybrid EEG-EMG BCI able to describe *good* functional recovery.

References

[1] ‘State of the Nation: stroke statistics’, *Stroke Association*, 03-Mar-2015. [Online]. Available: https://www.stroke.org.uk/resources/state-nation-stroke-statistics.

[2] G. J. Hankey, ‘Stroke’, *The Lancet*, vol. 389, no. 10069, pp. 641–654, Feb. 2017.

[3] A. Riccio *et al.*, ‘Chapter 12 - Interfacing brain with computer to improve communication and rehabilitation after brain damage’, in *Progress in Brain Research*, vol. 228, D. Coyle, Ed. Elsevier, 2016, pp. 357–387.

[4] J. Wolpaw and E. W. Wolpaw, Eds., *Brain-Computer Interfaces: Principles and Practice*. Oxford, New York: Oxford University Press, 2012.

[5] N. Sharma and J.-C. Baron, ‘Does motor imagery share neural networks with executed movement: a multivariate fMRI analysis’, *Front. Hum. Neurosci.*, vol. 7, p. 564, 2013.

[6] M. A. Dimyan and L. G. Cohen, ‘Neuroplasticity in the context of motor rehabilitation after stroke’, *Nat. Rev. Neurol.*, vol. 7, no. 2, pp. 76–85, Feb. 2011.

[7] F. Pichiorri *et al.*, ‘Sensorimotor rhythm-based brain-computer interface training: the impact on motor cortical

responsiveness', *J. Neural Eng.*, vol. 8, no. 2, p. 025020, Apr. 2011.

[8] F. Cincotti *et al.*, 'EEG-based brain-computer interface to support post-stroke motor rehabilitation of the upper limb', presented at the Proceedings of the Annual International Conference of the IEEE Engineering in Medicine and Biology Society, EMBS, 2012, pp. 4112–4115.

[9] F. Pichiorri *et al.*, 'Brain-computer interface boosts motor imagery practice during stroke recovery', *Ann. Neurol.*, vol. 77, no. 5, pp. 851–865, 2015.

[10] D. J. Gladstone, C. J. Danells, and S. E. Black, 'The fugl-meyer assessment of motor recovery after stroke: a critical review of its measurement properties', *Neurorehabil. Neural Repair*, vol. 16, no. 3, pp. 232–240, Sep. 2002.

[11] O. F. do Nascimento, K. D. Nielsen, and M. Voigt, 'Movement-related parameters modulate cortical activity during imaginary isometric plantar-flexions', *Exp. Brain Res.*, vol. 171, no. 1, pp. 78–90, May 2006.

[12] H. Shibasaki and M. Hallett, 'What is the Bereitschaftspotential?', *Clin. Neurophysiol. Off. J. Int. Fed. Clin. Neurophysiol.*, vol. 117, no. 11, pp. 2341–2356, Nov. 2006.

[13] R. Cunnington, R. Iansek, J. L. Bradshaw, and J. G. Phillips, 'Movement-related potentials associated with movement preparation and motor imagery', *Exp. Brain Res.*, vol. 111, no. 3, pp. 429–436, Oct. 1996.

[14] H. Shibasaki, G. Barrett, E. Halliday, and A. M. Halliday, 'Cortical potentials associated with voluntary foot movement in man', *Electroencephalogr. Clin. Neurophysiol.*, vol. 52, no. 6, pp. 507–516, Dec. 1981.

[15] D. O. Hebb, *The Organization of Behavior: A Neuropsychological Theory*, 1 edizione. Mahwah, N.J: Psychology Press, 2002.

[16] N. Mrachacz-Kersting *et al.*, 'Efficient neuroplasticity induction in chronic stroke patients by an associative brain-computer interface', *J. Neurophysiol.*, vol. 115, no. 3, pp. 1410–1421, Mar. 2016.

[17] N. Mrachacz-Kersting, S. R. Kristensen, I. K. Niazi, and D. Farina, 'Precise temporal association between cortical potentials evoked by motor imagination and afference induces cortical plasticity', *J. Physiol.*, vol. 590, no. 7, pp. 1669–1682, Apr. 2012.

[18] I. Choi, I. Rhiu, Y. Lee, M. H. Yun, and C. S. Nam, 'A systematic review of hybrid brain-computer interfaces: Taxonomy and usability perspectives', *PloS One*, vol. 12, no. 4, p. e0176674, 2017.

[19] J. d. R. Millán *et al.*, 'Combining Brain–Computer Interfaces and Assistive Technologies: State-of-the-Art and Challenges', *Front. Neurosci.*, vol. 4, Sep. 2010.

[20] G. Müller-Putz *et al.*, 'Towards Noninvasive Hybrid Brain–Computer Interfaces: Framework, Practice, Clinical Application, and Beyond', *Proc. IEEE*, vol. 103, no. 6, pp. 926–943, Jun. 2015.

[21] A. Riccio *et al.*, 'Hybrid P300-based brain-computer interface to improve usability for people with severe motor disability: electromyographic signals for error correction during a spelling task', *Arch. Phys. Med. Rehabil.*, vol. 96, no. 3 Suppl, pp. S54-61, Mar. 2015.

[22] M. Rohm *et al.*, 'Hybrid brain-computer interfaces and hybrid neuroprostheses for restoration of upper limb functions in individuals with high-level spinal cord injury', *Artif. Intell. Med.*, vol. 59, no. 2, pp. 133–142, Oct. 2013.

[23] U. Chaudhary, N. Birbaumer, and A. Ramos-Murguialday, 'Brain-computer interfaces for communication and rehabilitation', *Nat. Rev. Neurol.*, vol. 12, no. 9, pp. 513–525, 2016.

[24] M. Kawakami *et al.*, 'A new therapeutic application of brain-machine interface (BMI) training followed by hybrid assistive neuromuscular dynamic stimulation (HANDS) therapy for patients with severe hemiparetic

stroke: A proof of concept study', *Restor. Neurol. Neurosci.*, vol. 34, no. 5, pp. 789–797, 21 2016.

[25] F. Lotte *et al.*, 'A review of classification algorithms for EEG-based brain-computer interfaces: a 10 year update', *J. Neural Eng.*, vol. 15, no. 3, p. 031005, Jun. 2018.

[26] H. Bashashati, R. K. Ward, G. E. Birch, and A. Bashashati, 'Comparing Different Classifiers in Sensory Motor Brain Computer Interfaces', *PLoS ONE*, vol. 10, no. 6, Jun. 2015.

[27] D. Steyrl, R. Scherer, J. Faller, and G. R. Müller-Putz, 'Random forests in non-invasive sensorimotor rhythm brain-computer interfaces: a practical and convenient non-linear classifier', *Biomed. Tech. (Berl)*, vol. 61, no. 1, pp. 77–86, Feb. 2016.

[28] D. J. McFarland, L. M. McCane, S. V. David, and J. R. Wolpaw, 'Spatial filter selection for EEG-based communication', *Electroencephalogr. Clin. Neurophysiol.*, vol. 103, no. 3, pp. 386–394, 1997.

[29] D. J. McFarland, 'The advantages of the surface Laplacian in brain-computer interface research', *Int. J. Psychophysiol.*, vol. 97, no. 3, pp. 271–276, 2015.

[30] F. Cincotti *et al.*, 'Non-invasive brain-computer interface system: Towards its application as assistive technology', *Brain Res. Bull.*, vol. 75, no. 6, pp. 796–803, 2008.

[31] G. Schalk, D. J. McFarland, T. Hinterberger, N. Birbaumer, and J. R. Wolpaw, 'BCI2000: A general-purpose brain-computer interface (BCI) system', *IEEE Trans. Biomed. Eng.*, vol. 51, no. 6, pp. 1034–1043, 2004.

[32] D. J. McFarland, A. T. Lefkowicz, and J. R. Wolpaw, 'Design and operation of an EEG-based brain-computer interface with digital signal processing technology', *Behav. Res. Methods Instrum. Comput.*, vol. 29, no. 3, pp. 337–345, Sep. 1997.

[33] J. O. Rawlings, S. G. Pantula, and D. A. Dickey, *Applied Regression Analysis: A Research Tool*, 2nd ed. New York: Springer-Verlag, 1998.

[34] D. J. Krusienski *et al.*, 'A comparison of classification techniques for the P300 Speller', *J. Neural Eng.*, vol. 3, no. 4, pp. 299–305, Dec. 2006.

[35] T. Fawcett, 'An introduction to ROC analysis', *Pattern Recognit. Lett.*, vol. 27, no. 8, pp. 861–874, Jun. 2006.

[36] A. Hyvärinen and E. Oja, 'Independent component analysis: algorithms and applications', *Neural Netw. Off. J. Int. Neural Netw. Soc.*, vol. 13, no. 4–5, pp. 411–430, Jun. 2000.

[37] D. J. Krusienski, D. J. McFarland, and J. R. Wolpaw, 'Value of amplitude, phase, and coherence features for a

sensorimotor rhythm-based brain-computer interface', *Brain Res. Bull.*, vol. 87, no. 1, pp. 130–134, 2012.

[38] K. K. Ang, Z. Y. Chin, C. Wang, C. Guan, and H. Zhang, 'Filter Bank Common Spatial Pattern Algorithm on BCI Competition IV Datasets 2a and 2b', *Front. Neurosci.*, vol. 6, 2012.

[39] T. N. Lal *et al.*, 'Support vector channel selection in BCI', *IEEE Trans. Biomed. Eng.*, vol. 51, no. 6, pp. 1003–1010, Jun. 2004.

[40] R. Corralejo, R. Hornero, and D. Álvarez, 'Feature selection using a genetic algorithm in a motor imagery-based Brain Computer Interface', *Conf. Proc. Annu. Int. Conf. IEEE Eng. Med. Biol. Soc. IEEE Eng. Med. Biol. Soc. Annu. Conf.*, vol. 2011, pp. 7703–7706, 2011.

[41] D. J. McFarland, W. A. Sarnacki, and J. R. Wolpaw, 'Electroencephalographic (EEG) control of three-dimensional movement', *J. Neural Eng.*, vol. 7, no. 3, p. 036007, Jun. 2010.

[42] '(PDF) BCI Software Platforms', *ResearchGate*. [Online]. Available: https://www.researchgate.net/publication/279261462_BCI_Software_Platforms.

[43] A. Kübler *et al.*, 'The User-Centered Design as Novel Perspective for Evaluating the Usability of BCI-Controlled

Applications', *PLOS ONE*, vol. 9, no. 12, p. e112392, Dec. 2014.

[44] G. Morone *et al.*, 'Proof of principle of a brain-computer interface approach to support poststroke arm rehabilitation in hospitalized patients: design, acceptability, and usability', *Arch. Phys. Med. Rehabil.*, vol. 96, no. 3 Suppl, pp. S71-78, Mar. 2015.

[45] I. K. Niazi, N. Jiang, O. Tiberghien, J. F. Nielsen, K. Dremstrup, and D. Farina, 'Detection of movement intention from single-trial movement-related cortical potentials', *J. Neural Eng.*, vol. 8, no. 6, 2011.

[46] N. Jiang, L. Gizzi, N. Mrachacz-Kersting, K. Dremstrup, and D. Farina, 'A brain-computer interface for single-trial detection of gait initiation from movement related cortical potentials', *Clin. Neurophysiol. Off. J. Int. Fed. Clin. Neurophysiol.*, vol. 126, no. 1, pp. 154–159, Jan. 2015.

[47] R. Xu, N. Jiang, C. Lin, N. Mrachacz-Kersting, K. Dremstrup, and D. Farina, 'Enhanced low-latency detection of motor intention from EEG for closed-loop brain-computer interface applications', *IEEE Trans. Biomed. Eng.*, vol. 61, no. 2, pp. 288–296, 2014.

[48] C. Lin, B. Wang, N. Jiang, R. Xu, N. Mrachacz-Kersting, and D. Farina, 'Discriminative Manifold Learning Based Detection of Movement-Related Cortical Potentials', *IEEE*

Trans. Neural Syst. Rehabil. Eng., vol. 24, no. 9, pp. 921–927, Sep. 2016.

[49] C. Vidaurre, C. Sannelli, K.-R. Müller, and B. Blankertz, 'Machine-learning-based coadaptive calibration for brain-computer interfaces', *Neural Comput.*, vol. 23, no. 3, pp. 791–816, Mar. 2011.

[50] M. M.-C. Vidovic, H.-J. Hwang, S. Amsuss, J. M. Hahne, D. Farina, and K.-R. Muller, 'Improving the Robustness of Myoelectric Pattern Recognition for Upper Limb Prostheses by Covariate Shift Adaptation', *IEEE Trans. Neural Syst. Rehabil. Eng. Publ. IEEE Eng. Med. Biol. Soc.*, vol. 24, no. 9, pp. 961–970, 2016.

[51] M. Jochumsen, I. K. Niazi, N. Mrachacz-Kersting, D. Farina, and K. Dremstrup, 'Detection and classification of movement-related cortical potentials associated with task force and speed', *J. Neural Eng.*, vol. 10, no. 5, p. 056015, Oct. 2013.

[52] C. Bibián, E. López-Larraz, N. Irastorza-Landa, N. Birbaumer, and A. Ramos-Murguialday, 'Evaluation of filtering techniques to extract movement intention information from low-frequency EEG activity', in *2017 39th Annual International Conference of the IEEE Engineering in Medicine and Biology Society (EMBC)*, 2017, pp. 2960–2963.

[53] D. Cai, X. He, K. Zhou, and J. Han, ‘Locality Sensitive Discriminant Analysis’, p. 6.

[54] Q. Wang and L. Zhang, ‘Least squares online linear discriminant analysis’, *Expert Syst. Appl.*, vol. 39, no. 1, pp. 1510–1517, Jan. 2012.

[55] K. S. Sunnerhagen, ‘Predictors of Spasticity After Stroke’, *Curr. Phys. Med. Rehabil. Rep.*, vol. 4, pp. 182–185, 2016.

[56] L. M. McPherson *et al.*, ‘Properties of the motor unit action potential shape in proximal and distal muscles of the upper limb in healthy and post-stroke individuals’, presented at the Proceedings of the Annual International Conference of the IEEE Engineering in Medicine and Biology Society, EMBS, 2016, vol. 2016-October, pp. 335–339.

[57] X. Li, A. Holobar, M. Gazzoni, R. Merletti, W. Z. Rymer, and P. Zhou, ‘Examination of Poststroke Alteration in Motor Unit Firing Behavior Using High-Density Surface EMG Decomposition’, *IEEE Trans. Biomed. Eng.*, vol. 62, no. 5, pp. 1242–1252, May 2015.

[58] L. C. Miller, C. K. Thompson, F. Negro, C. J. Heckman, D. Farina, and J. P. A. Dewald, ‘High-density surface EMG decomposition allows for recording of motor unit discharge from proximal and distal flexion synergy muscles simultaneously in individuals with stroke’,

presented at the 2014 36th Annual International Conference of the IEEE Engineering in Medicine and Biology Society, EMBC 2014, 2014, pp. 5340–5344.

[59] M. Spüler, N. Irastorza-Landa, A. Sarasola-Sanz, and A. Ramos-Murguialday, 'Extracting Muscle Synergy Patterns from EMG Data Using Autoencoders', in *Artificial Neural Networks and Machine Learning – ICANN 2016*, 2016, pp. 47–54.

[60] J. Roh, W. Z. Rymer, E. J. Perreault, S. B. Yoo, and R. F. Beer, 'Alterations in upper limb muscle synergy structure in chronic stroke survivors', *J. Neurophysiol.*, vol. 109, no. 3, pp. 768–781, 2013.

[61] V. C. K. Cheung *et al.*, 'Muscle synergy patterns as physiological markers of motor cortical damage', *Proc. Natl. Acad. Sci. U. S. A.*, vol. 109, no. 36, pp. 14652–14656, 2012.

[62] P. Tropea, V. Monaco, M. Coscia, F. Posteraro, and S. Micera, 'Effects of early and intensive neuro-rehabilitative treatment on muscle synergies in acute post-stroke patients: a pilot study', *J. NeuroEngineering Rehabil.*, vol. 10, p. 103, Oct. 2013.

[63] 'Standards for suface electromyography: The European project Surface EMG for non-invasive assessment of muscles (SENIAM) | Request PDF', *ResearchGate*. [Online].

Available: https://www.researchgate.net/publication/228486725_Standards_for_suface_electromyography_The_European_project_Surface_EMG_for_non-invasive_assessment_of_muscles_SENIAM.

[64] N. W. Willigenburg, A. Daffertshofer, I. Kingma, and J. H. van Dieën, 'Removing ECG contamination from EMG recordings: a comparison of ICA-based and other filtering procedures', *J. Electromyogr. Kinesiol. Off. J. Int. Soc. Electrophysiol. Kinesiol.*, vol. 22, no. 3, pp. 485–493, Jun. 2012.

[65] J. Chae, G. Yang, B. K. Park, and I. Labatia, 'Delay in initiation and termination of muscle contraction, motor impairment, and physical disability in upper limb hemiparesis', *Muscle Nerve*, vol. 25, no. 4, pp. 568–575, Apr. 2002.

[66] S. Solnik, P. Rider, K. Steinweg, P. DeVita, and T. Hortobágyi, 'Teager–Kaiser energy operator signal conditioning improves EMG onset detection', *Eur. J. Appl. Physiol.*, vol. 110, no. 3, pp. 489–498, Oct. 2010.

[67] P. W. Hodges and B. H. Bui, 'A comparison of computer-based methods for the determination of onset of muscle contraction using electromyography', *Electroencephalogr. Clin. Neurophysiol.*, vol. 101, no. 6, pp. 511–519, Dec. 1996.

[68] X. Li, P. Zhou, and A. S. Aruin, 'Teager-Kaiser energy operation of surface EMG improves muscle activity onset detection', *Ann. Biomed. Eng.*, vol. 35, no. 9, pp. 1532–1538, Sep. 2007.

[69] A. Burden, 'How should we normalize electromyograms obtained from healthy participants? What we have learned from over 25 years of research', *J. Electromyogr. Kinesiol. Off. J. Int. Soc. Electrophysiol. Kinesiol.*, vol. 20, no. 6, pp. 1023–1035, Dec. 2010.

[70] R. N. Barker, S. Brauer, and R. Carson, 'Training-induced changes in the pattern of triceps to biceps activation during reaching tasks after chronic and severe stroke', *Exp. Brain Res.*, vol. 196, no. 4, pp. 483–496, 2009.

Appendix A - General software information

The analysis, presented in the thesis, were performed in the MATLAB environment (The MathWorks, Inc., Natick, Massachusetts, USA) by customized scripts. Statistical analyses were performed by STATISTICA (Stat Soft. Inc., Tulsa, Oklahoma, USA).

Appendix B - Stroke patients dataset

Stroke patient data, analysed in the PhD thesis, were previously collected in the context of the randomized controlled trial in [9]. The study was approved by the IRCCS Santa Lucia Foundation (Rome, Italy) ethics board (Prot. CE/AG4-PROG.244-105) and written informed consent was obtained for each patient.

The main characteristics of the dataset are shown below.

Participants

Twenty-eight stroke patients were enrolled from those admitted to three stroke neurorehabilitation units of the Santa Lucia Foundation. All subjects were evaluated from the clinical point of view, as described in [9], and following inclusion criteria were applied:

- a history of first-ever unilateral, cortical, subcortical, or mixed stroke, caused by ischemia or haemorrhage that occurred 6 weeks to 6 months prior to study inclusion;
- hemiplegia/hemiparesis caused by the stroke;
- age between 18 and 80 years.

Exclusion criteria were the presence of chronic disabling diseases, such as orthopaedic injuries that could impair reaching or grasping; spasticity of the shoulder, elbow, or wrist, scored 4 or 5 on the Modified Ashworth Scale (MAS) and a Mini-Mental State Examination score less than 24. Subjects with severe hemispatial neglect, severe aphasia, and apraxia were excluded [9].

Intervention

All patients received the standard treatment for stroke in terms of medical care and rehabilitation for approximately 3 hours per day.

Fourteen patients received BCI-supported therapy; thus, the intervention was intended as add-on therapy. This group of patients received 1 month of BCI-supported MI training with 3 weekly sessions. The other group received equally intensive MI training without BCI assistance. Patients were assigned to BCI-assisted MI training or no-BCI assisted MI training interventions by blind randomized allocation.

Experimental protocol

Pre- and Post-Intervention assessment

All subjects were evaluated before (in this work called Pre) and after (Post) the interventions (see Intervention section). In all subjects an extensive neurophysiological assessment was conducted by high-density EEG. EMG signals were simultaneously collected from upper limb muscles of twelve subjects.

During the acquisition all subjects were comfortably seated in an armchair in a dimly lit room with their upper limbs resting on a desk. Visual cues were presented on a screen on the desk.

The sessions (Pre and Post) were divided into runs. Each run comprised 30 trials (15±1 rest, 15±1 experimental task). Each run was dedicated to a specific task that involved subject's unaffected or affected hand. The total trial duration was 7 seconds with an inter-trial interval of 3.5 seconds. Each trial began with a cursor appearing in the lower centre of the screen and moving on a line toward the top at constant velocity. During the rest trial no target appeared on the screen. In the experimental task trials, a green rectangle appeared at the top of the screen; its width was 100% of the screen width and its

height approximately equal to 57% of that of the screen (occupying the last 4 seconds of the cursor's trajectory, i.e. of the trial). The subject was instructed to start the experimental task when the cursor reached the green rectangle and continue it until the end of its trajectory (Figure 23).

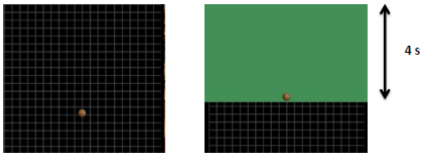

Figure 23 - Subject interface, implemented in BCI2000 [31], that guides subjects in the run. *Left panel,* Rest trial. *Right panel,* task trial. The patient was instructed to start the experimental task when the cursor reached the green rectangle and continue it until the end of its trajectory.

During the rest trials, subjects were asked to watch the cursor's movement on the screen. During the experimental task trials, subjects were instructed by the therapist to perform the movement imagery (kinesthetic MI) or the movement execution (attempt of execution) of the grasping (hand closing) or finger extension (hand opening) movement with their unaffected or affected upper limb. Each combination was acquired in a separate run.

Intervention assessment

The neurophysiological assessment of subjects who received the BCI-supported MI training intervention was conducted by high-density EEG. During the acquisition subjects were seated on a comfortable chair (or directly on their wheelchair) with their hands and forearms resting on a desk. Each training session comprised four or eight runs (20 trials for each run) depending on the subject's physical ability. Each trial included a rest period of 4 seconds and a task period of maximally 10 seconds. During the task period, subjects were asked to perform only the grasping or finger extension (acquired in separate runs) movement imagination of the paralyzed hand [44].

Experimental set-up

Pre- and Post-Intervention assessment

Scalp EEG potentials were collected from 61 electrodes, assembled on an electrode cap (according to an extension of the 10–20 International System, linked ears reference, mastoid ground) and bandpass filtered between 0.1 and 70Hz. EMG signals were collected from 12 muscles (6 muscles for each upper limb): flexor and extensor digitorum, long head of the biceps brachii, lateral head of the triceps brachii, lateral deltoid

and pectoralis major. For each muscle two surface electrodes were placed on the muscle belly (inter-electrode distance range [30-50] mm). Signals were recorded in monopolar fashion (reference electrode placed on the elbow lateral epicondylitis). All signals were digitalized at 200 Hz and amplified by a commercial EEG system (BrainAmp; Brain Products, Gilching, Germany).

Intervention assessment

Scalp EEG potentials were collected from 31 electrodes distributed over the scalp centre-parietal regions (FC5, FC3, FC1, FCz, FC2, FC4, FC6, C5, C3, C1, Cz, C2, C4, C6, CP5, CP3, CP1, CPz, CP2, CP4, CP6, P5, P3, P1, Pz, P2, P4, P6, PO3, POz, PO4), digitalized at 200 Hz and amplified by a commercial EEG system [44].

List of publications

[1] E. **Colamarino**, F. Pichiorri, D. Mattia, F. Cincotti (2019), "Bipolar filters improve usability of Brain-Computer Interface technology in post-stroke motor rehabilitation", in: Masia L., Micera S., Akay M., Pons J. (eds) Converging Clinical and Engineering Research on Neurorehabilitation III. ICNR 2018 (Pisa, Italia). Biosystems & Biorobotics, vol 21. Springer, Cham. DOI: 10.1007/978-3-030-01845-0_183

[2] F. Pichiorri, E. **Colamarino**, F. Cincotti, D. Mattia (2019), "An All-in-One BCI-Supported Motor Imagery Training Station: Validation in a Real Clinical Setting with Chronic Stroke Patients." In: Masia L., Micera S., Akay M., Pons J. (eds) Converging Clinical and Engineering Research on Neurorehabilitation III. ICNR 2018 (Pisa, Italia). Biosystems & Biorobotics, vol 21. Springer, Cham. DOI: 10.1007/978-3-030-01845-0_177

[3] F. Pichiorri, E. **Colamarino**, F. Cincotti, D. Mattia, “Brain-computer interface technology for upper limb rehabilitation after stroke: a translational effort”, Meeting Abstract of the 4th Congress of the European Academy of Neurology, June 16-19 2018, Lisbon (Portugal). European Journal of Neurology, Vol. 25, Supp 2, pag. 50.

[4] E. **Colamarino**, F. Pichiorri, D. Mattia, F. Cincotti, "Semiautomatic physiologically-driven feature selection improves the usability of a brain computer interface system in post-stroke motor rehabilitation", Abstract Book of the Seventh International BCI Meeting: “BCIs: not getting lost in Translation”, May 21-25 2018, Pacific Grove (California, USA), pag. 96-97

[5] E. **Colamarino**, F. Pichiorri, D. Mattia, F. Cincotti, "Spatial filters selection towards a rehabilitation BCI", Proceedings of the 7th Graz Brain-Computer Interface Conference: “From Vision to Reality”, September 18-22 2017, Graz (Austria), pag. 92-96. DOI: 10.3217/978-3-85125-533-1-18

[6] E. **Colamarino**, F. Pichiorri, F. Schettini, M. Martinoia, D. Mattia, F. Cincotti, "GUIDER: a GUI for semiautomatic, physiologically driven EEG feature selection for a rehabilitation BCI", Proceedings of the 7th Graz Brain-Computer Interface Conference: “From Vision to Reality”, September 18-22 2017, Graz (Austria), pag. 97-101. DOI: 10.3217/978-3-85125-533-1-19

[7] F. Pichiorri, E. **Colamarino**, D. Mattia, F. Cincotti, "The Promotoer: a successful story of translational research in BCI for motor rehabilitation", Proceedings of the 7th Graz Brain-Computer Interface Conference: “From Vision to Reality”,

September 18-22 2017, Graz (Austria), pag. 410-413. DOI: 10.3217/978-3-85125-533-1-75

[8] E. **Colamarino**, F. Pichiorri, D. Mattia, F. Cincotti, "Neurophysiological constraints of control parameters for a brain computer interface system to support post-stroke motor rehabilitation",

Proceedings of the School & Symposium on Advanced Neurorehabilitation, September 17-22 2017, Baiona (Spain)

[9] E. **Colamarino**, E. Merlo, G. Boccia, J. Toppi, D. Mattia, F. Cincotti, "Concentric-ring electrodes reduce crosstalk in surface EMG", Proceedings of the 5th Conference of the National Group of Bioengineering, June 20-22 2016, Naples (Italy)

[10] F. Schettini, M. Martinoia, F. Pichiorri, E. **Colamarino**, D. Mattia, F. Cincotti "Automatic features selection in BCI-supported motor imagery practice for stroke rehabilitation", Proceedings of the 5th Conference of the National Group of Bioengineering, June 20-22 2016, Naples (Italy)

List of funding and awards

2018 October	**Grant** (as Principal Investigator) for 1-year project “Avvio alla Ricerca” (AR11816436CA41E5) titled “Synergies-based real-time monitoring to improve post-stroke rehabilitation” received by Sapienza University of Rome
2018 March	**Student Award** to attend the 7th International BCI Meeting “BCIs: Not Getting Lost in Translation (21-25 May 2018, Asilomar Conference Center in Pacific Grove, California, (USA), financed by the National Institutes of Health and the National Science Foundation with the support of IEEE and OpenBCI
2017 December	Mobility Projects Call for Research Doctorates: **Grant** for the project titled “Motor Recovery supported by hybrid Brain-Computer Interface and complex network theory” received by Sapienza University of Rome

2017 July	**Grant** (as Principal Investigator) for 1-year project “Avvio alla Ricerca” (AR11715C823D7492) titled “Multimodal classification of upper limb movements during post-stroke rehabilitation” received by Sapienza University of Rome